

STABLE SPIN HALL-LITTLEWOOD SYMMETRIC FUNCTIONS, COMBINATORIAL IDENTITIES, AND HALF-SPACE YANG-BAXTER RANDOM FIELD

KAILUN CHEN AND XIANG-MAO DING

ABSTRACT. Stable spin Hall-Littlewood symmetric polynomials labeled by partitions were recently introduced by Borodin and Wheeler in the context of higher spin six vertex models, which are one-parameter deformation of the Hall-Littlewood polynomials. We present a new combinatorial definition for the stable spin Hall-Littlewood polynomials, and derive a series of new combinatorial identities, including the skew Littlewood identity, refined Cauchy identity and refined Littlewood identity.

Employing bijectivisation of summation identities, Bufetov and Petrov introduced local stochastic moves based on the Yang-Baxter equation. Combining the skew Littlewood identity and these moves, we introduce the half-space Yang-Baxter random field for stable spin Hall-Littlewood polynomials. We match the lengths of the partitions in this field with a new dynamic version of stochastic six vertex model in the half-quadrant, which can be mapped to a dynamic version of discrete-time interacting particle system on the half-line with an open boundary.

CONTENTS

1. Introduction	2
1.1. Overview	2
1.2. Notation	4
1.3. Outline	4
Acknowledgments	4
2. Stable spin Hall-Littlewood symmetric functions	4
2.1. Higher spin six vertex model and vertex weights	5
2.2. The first definition	6
2.3. The second definition	8
2.4. The equivalence of the two definitions	8
3. Combinatorial identities from Integrability	11
3.1. Integrability of the higher spin six vertex model	12
3.2. Skew Cauchy identity	12
3.3. Skew Littlewood identity	14
3.4. Refined Cauchy identity	17
3.5. Refined Littlewood identity	19
4. Half-space Random field	21
4.1. Skew Cauchy-Littlewood structure	21
4.2. Half-space Yang-Baxter random field	22
4.3. Sampling a half-space random field via the Markov transition operators	24
4.4. Construction of the bulk transition operators	25

4.5. Construction of the boundary transition operators	28
4.6. Evolution of the lengths of the partitions	29
4.7. A dynamic stochastic six vertex model in a half-quadrant	30
References	33

1. INTRODUCTION

1.1. **Overview.** Integrable lattice models [Bax82] have been found to provide a framework for simultaneously accessing the theory of symmetric functions and probability. In the symmetric function aspect, more and more kinds of symmetric functions have been realized in the integrable lattice models. In this setting, lots of combinatorial properties of corresponding symmetric functions can be explored. There is a great deal of literature on this subject, and we will not list them all here, but recommend the article [ABW21] for readers' reference, and it has an excellent summary. In the probability aspect, the integrability of numbers of probabilistic models in the KPZ universality class [KPZ86] comes down to the algebraic structure in the integrable lattice model. We refer to [Kor21] and references therein.

In this paper, we focus on the higher spin six vertex model, which was introduced in [Bor17] to define the (non-stable) spin Hall-Littlewood symmetric functions. From the Yang-Baxter integrability, the skew Cauchy identity and symmetrization formulas are derived, which imply spectral biorthogonality and spatial biorthogonality, respectively. Subsequently, a series of related works mushroomed. A stochastic fused version of a higher six vertex model was introduced in [CP16], which has nice probabilistic properties. On one hand, the Markov dualities and the Bethe Ansatz eigenfunctions admit a nested contour integral formulas for moments and the Fredholm determinant formulas for Laplace-type transforms. On the other hand, many exactly solvable models in the KPZ Universality class can be viewed as the degenerate cases of stochastic fused version of higher six vertex models: such as ASEP, stochastic six vertex model, q -TASEP, q -Hahn particle system and various directed polymer. Note that there are certain degrees of flexibility in the Yang-Baxter equation, an inhomogeneous version of stochastic higher six vertex model and an inhomogeneous version of spin Hall-Littlewood symmetric functions was introduced in [BP18]. Therein, the symmetric function method was developed: one can identify the expectation of some special observables with a single evaluation of the inhomogeneous spin Hall-Littlewood symmetric functions, and the integral representation for the latter leads to the desired integral expression. By a direct comparison of integral representations, the relationship of an inhomogeneous version of stochastic higher six vertex model and Macdonald measure [BC14] was found in [Bor18], which can be used for asymptotic analysis. Inspired by the success of Macdonald difference operators [Mac95] in Macdonald processes [BC14], the difference operators for the spin Hall-Littlewood symmetric functions was explored in [Dim18] to extract various correlation functions, which are suitable for asymptotic analysis. The relationship between an inhomogeneous stochastic higher spin six vertex model and the Macdonald processes has also been explored at the q -Whittaker and Hall-Littlewood level in [OP17, BBW16]. The story doesn't end here. A new stage – spin Hall-Littlewood Yang-Baxter field was introduced in [BP19], which relates a series of novel probabilistic models to the higher spin six vertex model, including the dynamic versions of the stochastic six vertex model and ASEP. In terms of combinatorial properties,

the refined Cauchy identity and refined Littlewood identity for inhomogeneous spin Hall-Littlewood symmetric functions have been introduced recently in [Pet20, Gav21]. Moreover, the refined Cauchy identity built a bridge between the inhomogeneous spin Hall-Littlewood symmetric functions and the interpolation Macdonald polynomials [Ols19, Cue18]

In the process of exploring a higher level of symmetric function, a stable version of spin Hall-Littlewood symmetric functions was introduced in [GdGW17]. But there is not so much discussion about stable spin Hall-Littlewood symmetric functions.¹ The Cauchy identity and a dual Cauchy identity was derived in [BW20]. A probabilistic application of *ssHL functions* was introduced in [BMP19] through the Yang-Baxter random fields, and the Fredholm determinant formulas for the Laplace-type transforms are performed by the difference operator.

Our goal in this paper is to develop further the combinatorial and probabilistic properties of the *ssHL functions* under the higher spin six vertex model, which have not been noticed so far. Here is a summary of our results.

- In [BW20], there are infinity arrows on the column 0 in the combinatorial definition of *ssHL functions*, which is not convenient for us to derive extra combinatorial identities. We give a new different definition for *ssHL functions* (see Definition 2.1), there we delete the column 0, and boundary conditions outside the first column become free (see Figure 4). We prove the equivalence of our definition and the one in [BW20]. The known combinatorial properties of *ssHL functions* can still be derived by our definition.
- By the new definition of the *ssHL functions* and Yang-Baxter integrability, we can derive a series of combinatorial identities in a uniform way: skew Cauchy identity (see Theorem 3.1), skew Littlewood identity (see Theorem 3.5), refined Cauchy identity (see Theorem 3.8), refined Littlewood identity (see Theorem 3.10). The skew Cauchy identity of *ssHL functions* have been obtained in [BW20] by an algebraic approach, but we use a combinatorial approach. The skew Littlewood identity of *ssHL functions* is first derived in this paper. Although the refined Cauchy identity and refined Littlewood identity of *ssHL functions* can be viewed as the degenerated case of (non-stable) inhomogeneous spin Hall-Littlewood polynomials(see remark 3.9 and remark 3.11), we can get these formulas in a more straightforward way.
- Up to now, the higher spin six vertex model can only hatch the full-space probabilistic models. For the first time, we include the half-space probabilistic models into this framework. Our approach is to construct a *half-space Yang-Baxter field* (see Definition 4.2), which is an extension of the (full-space) Yang-Baxter field in [BMP19]. The half-space Yang-Baxter field can be sampled by two kinds of Markov transition operators: bulk transition operators and boundary transition operators. Employing the skew Littlewood identity, we find that the bijectivisation of Yang-Baxter equation introduced in [BP19] can be used to construct both the bulk and boundary transition operators. Our construction provides a new dynamic evolution method for the random partitions in the half-quadrant, which is different from the one in [BBCS18, BBC20].
- We define a new dynamic version of stochastic six vertex model in a half-quadrant (see Definition 4.4). We match the joint distribution of the height function in the new dynamic vertex model with the joint distribution of the lengths of the random

¹We will abbreviate the name to *ssHL functions*.

partitions from the half-space Yang-Baxter field, such that we can explore the integrability of the new dynamic vertex model under the umbrella of half-space *ssHL process* (see the probability measure 4.2.2). Moreover, the new dynamic version of stochastic six vertex model in a half-quadrant can be mapped to a dynamic version of discrete-time interacting particle system on the half-line with an open boundary. (see Figure 22).

1.2. Notation. A partition λ is an infinite non-increasing sequence of non-negative integers $\lambda = (\lambda_1 \geq \lambda_2 \geq \dots \geq \lambda_n \geq \dots)$ with only finitely many non-zero elements. The non-zero elements λ_i are called the parts of λ . The number of parts is the length of λ , denoted by $\ell(\lambda)$. Denote by \mathbb{Y} the set of all partitions including the empty one $\lambda = \emptyset$ (by agreement, $\ell(\emptyset) = 0$). We say that μ and λ *interlace* (notation $\mu \prec \lambda$) if either one of the two are hold:

$$(1.2.1) \quad \begin{aligned} \ell(\lambda) = \ell(\mu) \text{ and } \mu_{\ell(\mu)} \leq \lambda_{\ell(\lambda)} \leq \dots \leq \lambda_2 \leq \mu_1 \leq \lambda_1, \\ \ell(\lambda) = \ell(\mu) + 1 \text{ and } \lambda_{\ell(\lambda)} \leq \mu_{\ell(\mu)} \leq \lambda_{\ell(\lambda)-1} \leq \dots \leq \lambda_2 \leq \mu_1 \leq \lambda_1. \end{aligned}$$

Sometimes it is convenient to use a notation which indicates the number of times each integer occurs as a part

$$(1.2.2) \quad \lambda = 1^{m_1} 2^{m_2} \dots$$

Such is saying that it is exactly m_i of the parts of λ are equal to i , $m_i = \#\{j : \lambda_j = i\}$. If all the λ_i are even, we say that partition λ is even. The conjugate of a partition λ is the partition λ' whose diagram is the transpose of the diagram λ obtained by reflection in the main diagonal, $\lambda'_i = \#\{j : \lambda_j \geq i\}$.

1.3. Outline. In section 2, we recall the higher spin six vertex model and give several different kinds of definitions of *ssHL functions*. In section 3, we introduce the integrability of higher spin six vertex model and derive a series of combinatorial identities for *ssHL functions*: skew Cauchy identity, skew Littlewood identity, refined Cauchy identity, refined Littlewood identity. In section 4, we introduce the half-space Yang-Baxter field associated with the skew Cauchy-Littlewood structure, which can be constructed by the Markov transition operators. We use the bijectivisation of the Yang-Baxter equation to construct the Markov transition operators, and relate the corresponding half-space Yang-Baxter random field to a dynamic version of stochastic six vertex model in a half-quadrant.

Acknowledgments. The financial supports from the Natural Science Foundation of China (NSFC, Grants 11775299) and National Key Research and Developing Program of China (NKRDP, Grants 2018YFB0704304) are gratefully acknowledged from one of the authors (Ding).

2. STABLE SPIN HALL-LITTLEWOOD SYMMETRIC FUNCTIONS

In this section, we give two equivalent definitions of *ssHL functions* in the frame of higher spin six vertex model [Bor17, BP18, BP16]. Section 2.1 introduces the higher spin six vertex model and related vertex weights. Section 2.2 gives the first definition of *ssHL functions* and their dual. One can find that the first definition is easily for us to derive a sequence of combinatorial identities in section 3. Section 2.3 gives the second definition of *ssHL functions* and their dual, which was first introduced in [BW20]. One can find that the second definition

is convenient for us to recognize the evolution of the lengths of the partitions in the half-space Yang-Baxter random field in section 4. We prove the equivalence of the above two definitions in section 2.4.

2.1. Higher spin six vertex model and vertex weights. Higher spin six vertex model is a square lattice model on certain domain of a plane. The square lattices are comprised of oriented horizontal and vertical lines. A point where a horizontal line and a vertical line intersect is called a vertex. A line segment between the vertices is called an edge. Every edge is assigned with oriented paths, the directions of the paths are the same as the line they live on. The paths directed to (respectively, be away from) the vertex are called the incoming paths (respectively, outgoing paths), and the number of incoming paths are the same as outgoing ones. We assume that the number of paths on the horizontal edges can be at most one, but no restriction on the vertical edge. Graphically, a vertex coated with a thin horizontal line and a thick vertical line. For a vertex, we assign a Boltzmann weight that depends on the type of the vertex and the number of incoming and outgoing paths. We list the three types of vertex and their Boltzmann weights [BW20] in Figure 1–3, here we use a capital letter and a small letter, to label the the number of paths in the vertical line and horizontal line, respectively. The two global fixed parameters are the quantization parameter q , and spin parameter s , respectively. The spectral parameter x is a local parameter which depends on the horizontal line it lives on. A configuration means an assignment of all the edges by the oriented paths, and the Boltzmann weight of a configuration is the product of the Boltzmann weights of all the vertices for the configuration. The partition function of the higher spin six vertex model is the sum of Boltzmann weights for all the possible configurations.

$L_{x,s}(I, j; K, \ell)$	$\frac{1 - sq^I}{1 - sx}$	$\frac{x - sq^I}{1 - sx}$	$\frac{1 - q^{I+1}}{1 - sx}$	$\frac{x(1 - s^2q^I)}{1 - sx}$

FIGURE 1. Type 1 vertex with grey line and SW \rightarrow NE oriented paths.

$M_{x,s}(I, j; K, \ell)$	$\frac{x - sq^I}{1 - sx}$	$\frac{1 - sq^I}{1 - sx}$	$\frac{x(1 - q^{I+1})}{1 - sx}$	$\frac{1 - s^2q^I}{1 - sx}$

FIGURE 2. Type 2 vertex with red line and SW \rightarrow NE oriented paths.

$M_{x,s}^*(I, j; K, \ell)$	$\frac{1 - sxq^I}{1 - sx}$	$\frac{x - sq^I}{1 - sx}$	$\frac{1 - s^2q^I}{1 - sx}$	$\frac{x(1 - q^{I+1})}{1 - sx}$

FIGURE 3. Type 3 vertex with red line and NW \rightarrow SE oriented paths.

To incorporate the partition functions in terms of linear operators, we introduce an algebraic setting with associating a vector space to each line. The vertical line associated with an infinite-dimensional vector space $V = \text{Span} \{|I\rangle\}_{I \in \mathbb{Z}_{\geq 0}}$ is called the local physical space, and the horizontal line associated with a two-dimensional vector space $W = \text{Span} \{|i\rangle\}_{i=0,1}$ is called the local auxiliary space. We will identify the number in the vector $|\cdot\rangle$ with the number of paths. Further, we construct the global physical space (respectively, global auxiliary space) by numbering each local physical space (respectively, local auxiliary space) a nonnegative integer and performing the tensor product.

2.2. The first definition. We consider the higher spin six vertex model on the domain $\mathbb{Z}_{\leq -1} \times \mathbb{Z}_{\leq -1}$. The global physical space is the tensor product of countably many local physical space: $V_1 \otimes V_2 \otimes V_3 \otimes \dots$, where each V_i is a copy of local vector space V , and the index number $i \geq 1$ is assigned to the vertical line with the abscissa $-i$. We only consider the global vector with finitely many nonzero local vectors, and denote this subspace by \mathbb{V} . Therefore, the linear space \mathbb{V} has the partition basis:

$$(2.2.1) \quad |\lambda\rangle = \bigotimes_{i=1}^{\infty} |K_i\rangle_i, \quad \lambda = 1^{K_1} 2^{K_2} \dots$$

where $|K_i\rangle_i$ is a local vector in the local vector space V_i , K_i means the number of the paths in the vertical line with abscissa $-i$. Similarly, one can define the dual partition vector in the dual vector space \mathbb{V}^*

$$(2.2.2) \quad \langle \mu | = \bigotimes_{i=1}^{\infty} \langle I_i |_i, \quad \mu = 1^{I_1} 2^{I_2} \dots$$

with the orthogonal relation $\langle \mu | \lambda \rangle = \delta_{\mu, \lambda}$ for all partitions μ, λ .

We now define two families of linear *row operators* acting on the partition vectors:

$$(2.2.3) \quad T_{\ell}(x) : \bigotimes_{i=1}^{\infty} |K_i\rangle_i \mapsto \sum_{I_1, I_2, I_3, \dots \in \mathbb{Z}_{\geq 0}} \left(x \rightarrow 0 \begin{array}{c} \dots \dots \dots K_3 \ K_2 \ K_1 \\ \uparrow \uparrow \uparrow \uparrow \uparrow \uparrow \\ \dots \dots \dots I_3 \ I_2 \ I_1 \end{array} \rightarrow \ell \right) \bigotimes_{i=1}^{\infty} |I_i\rangle_i, \quad \ell = 0, 1,$$

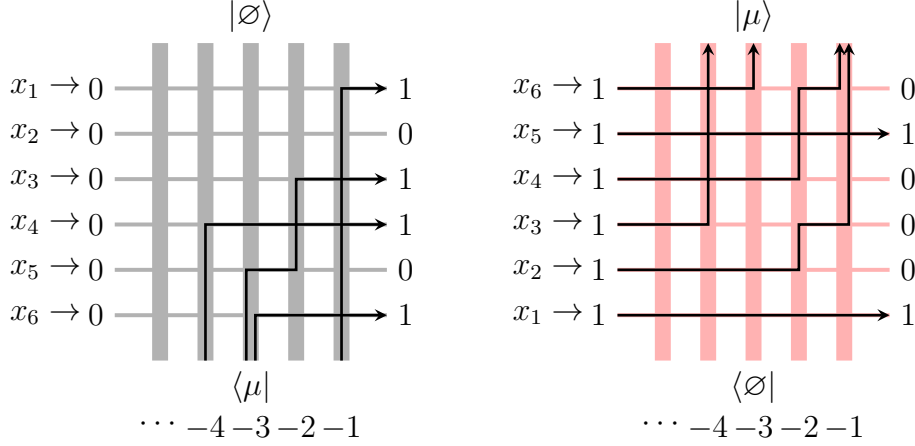


FIGURE 4. Left panel: a configuration of $f_\mu(x_1, \dots, x_6)$ with $\mu = (4, 3, 3, 1)$. Right panel: a configuration of $g_\mu(x_1, \dots, x_6)$ with $\mu = (4, 3, 1, 1)$.

(2.2.4)

$$T_\ell^*(x) : \bigotimes_{i=1}^{\infty} |K_i\rangle_i \mapsto \sum_{I_1, I_2, I_3, \dots \in \mathbb{Z}_{\geq 0}} \left(x \rightarrow 1 \begin{array}{c} \dots \dots \dots K_3 \ K_2 \ K_1 \\ \uparrow \uparrow \uparrow \uparrow \uparrow \\ \dots \dots \dots I_3 \ I_2 \ I_1 \end{array} \rightarrow \ell \right) \bigotimes_{i=1}^{\infty} |I_i\rangle_i, \quad \ell = 0, 1.$$

where the expansion coefficients in the sums are one-row partition functions in the higher-spin vertex models defined in Section 2.1, with vertex weights in Figure 1 and Figure 2. Using two sums of row operators,

$$(2.2.5) \quad \mathcal{T}(x) = T_0(x) + T_1(x),$$

$$(2.2.6) \quad \mathcal{T}^*(x) = T_0^*(x) + T_1^*(x),$$

we can give the first definition of (skew) *ssHL functions* and their dual:

Definition 2.1. For two fixed partitions λ and μ , we define the skew *ssHL functions* $f_{\mu/\lambda}(x_1, \dots, x_n)$ and their dual $g_{\mu/\lambda}(x_1, \dots, x_n)$, respectively as:

$$(2.2.7) \quad f_{\mu/\lambda}(x_1, \dots, x_n) := \langle \mu | \mathcal{T}(x_n) \cdots \mathcal{T}(x_2) \mathcal{T}(x_1) | \lambda \rangle,$$

$$(2.2.8) \quad g_{\mu/\lambda}(x_1, \dots, x_n) := \langle \lambda | \mathcal{T}^*(x_1) \mathcal{T}^*(x_2) \cdots \mathcal{T}^*(x_n) | \mu \rangle.$$

Note that the length of partition μ and λ satisfy $0 \leq \ell(\mu) - \ell(\lambda) \leq n$, and specially If $\lambda = \emptyset$, the non-skew version are

$$(2.2.9) \quad f_\mu(x_1, \dots, x_n) := \langle \mu | \mathcal{T}(x_n) \cdots \mathcal{T}(x_2) \mathcal{T}(x_1) | \emptyset \rangle,$$

$$(2.2.10) \quad g_\mu(x_1, \dots, x_n) := \langle \emptyset | \mathcal{T}^*(x_1) \mathcal{T}^*(x_2) \cdots \mathcal{T}^*(x_n) | \mu \rangle.$$

respectively, see Figure 4 for example.

The Definition 2.1 is a natural generalization of the vertex model definition of Hall-Littlewood polynomials in [BBW16].

2.3. The second definition. We can also view the partition basis (2.2.1) as a vector in a larger physical space $V_0 \otimes V_1 \otimes V_2 \otimes \cdots$ with $V_0 = \text{Span}\{|\infty\rangle\}$. Therefore, we consider the higher spin six vertex model on the domain $\mathbb{Z}_{\geq 0} \times \mathbb{Z}_{\geq 1}$. The index number $i \geq 0$ in the local physical space V_i assigns to the vertical line with the abscissa i . We still use the notation \mathbb{V} and $|\lambda\rangle$ to express the linear subspace which has the partition basis, the dual vector space \mathbb{V}^* and the dual partition basis is similar.

Similar with row operator (2.2.5) and (2.2.6), we define two linear *row operators* on the larger physical space $V_0 \otimes V_1 \otimes V_2 \otimes \cdots$ by the following way:

$$(2.3.1) \quad \tilde{\mathcal{T}}(x) : |\lambda\rangle \mapsto \sum_{\mu} \left(x \rightarrow 0 \begin{array}{c} \infty \quad K_1 \quad K_2 \quad K_3 \quad \dots \quad \dots \\ \downarrow \quad \downarrow \quad \downarrow \quad \downarrow \quad \downarrow \quad \downarrow \\ \infty \quad I_1 \quad I_2 \quad I_3 \quad \dots \quad \dots \end{array} \rightarrow 0 \right) |\mu\rangle.$$

$$(2.3.2) \quad \tilde{\mathcal{T}}^*(x) : |\lambda\rangle \mapsto \sum_{\mu} \left(x \rightarrow 1 \begin{array}{c} \infty \quad K_1 \quad K_2 \quad K_3 \quad \dots \quad \dots \\ \uparrow \quad \uparrow \quad \uparrow \quad \uparrow \quad \uparrow \quad \uparrow \\ \infty \quad I_1 \quad I_2 \quad I_3 \quad \dots \quad \dots \end{array} \rightarrow 0 \right) |\mu\rangle,$$

where $\lambda = 1^{K_1} 2^{K_2} \cdots$ and $\mu = 1^{I_1} 2^{I_2} \cdots$, the vertices in the one row partition function have the Boltzmann weights in Figure 1 and 3. We also define the Boltzmann weights of the vertices in the 0-th column have the following form:

$$(2.3.3) \quad \left(\begin{array}{c} \infty \\ \uparrow \\ 1 \rightarrow \ell \\ \infty \end{array} \right) = \left(\begin{array}{c} \infty \\ \downarrow \\ 0 \rightarrow \ell \\ \infty \end{array} \right) = x^\ell, \quad 0 \leq \ell \leq 1.$$

Employing the above operators, we can give the second definition of *ssHL functions* and their dual by substituting (2.3.1) for (2.2.5) and substituting (2.3.2) for (2.2.6) in definition 2.1, respectively. See Figure 5 for example. We refer to [BW20, BMP19] for more explanation.

2.4. The equivalence of the two definitions. We can prove the equivalence of the above two definitions of skew *ssHL functions* and their dual by checking:

$$(2.4.1) \quad \langle \mu | \mathcal{T}(x) | \lambda \rangle = \langle \mu | \tilde{\mathcal{T}}(x) | \lambda \rangle$$

$$(2.4.2) \quad \langle \lambda | \mathcal{T}^*(x) | \mu \rangle = \langle \lambda | \tilde{\mathcal{T}}^*(x) | \mu \rangle$$

For any given partition λ and μ , we only need to check (2.4.1) and (2.4.2) with the condition of $0 \leq \ell(\mu) - \ell(\lambda) \leq 1$, otherwise, the quantities on the two sides of the equations will vanish. We only prove (2.4.1), the proof of (2.4.2) is similar. In the partition function $\langle \mu | \mathcal{T}(x) | \lambda \rangle$, we denote the Boltzmann weight of the vertex with abscissa $-i$ by $\mathcal{T}_i(x)$. In the partition function $\langle \mu | \tilde{\mathcal{T}}(x) | \lambda \rangle$, we denote the Boltzmann weight of the vertex with abscissa i by $\tilde{\mathcal{T}}_i(x)$, and $\mathcal{T}_i(x)$ and $\tilde{\mathcal{T}}_i(x)$ have the following relation:

$$\mathcal{T}_i(x) = \begin{cases} \tilde{\mathcal{T}}_i(x), & m_i(\mu) = m_i(\lambda), \\ x \cdot \tilde{\mathcal{T}}_i(x), & m_i(\mu) > m_i(\lambda), \\ x^{-1} \cdot \tilde{\mathcal{T}}_i(x), & m_i(\mu) < m_i(\lambda). \end{cases}$$

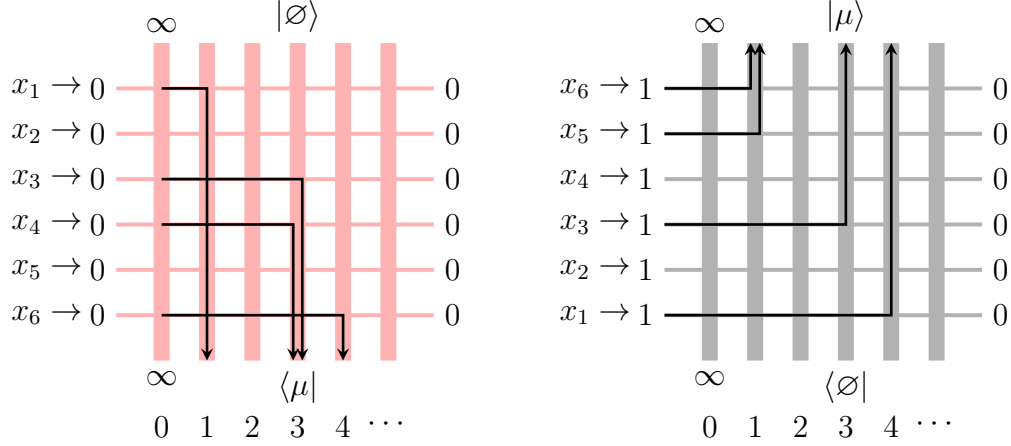


FIGURE 5. Left panel: a configuration of $f_\mu(x_1, \dots, x_6)$ with $\mu = (4, 3, 3, 1)$. Right panel: a configuration of $g_\mu(x_1, \dots, x_6)$ with $\mu = (4, 3, 1, 1)$.

where $m_i(\lambda) = \#\{j : \lambda_j = i\}$. If $\ell(\mu) = \ell(\lambda)$, we have $\#\{m_i(\mu) > m_i(\lambda)\} = \#\{m_i(\mu) < m_i(\lambda)\}$ and $\tilde{\mathcal{T}}_0(x) = 1$, (2.4.1) holds. As $\ell(\mu) = \ell(\lambda) + 1$, we have $\#\{m_i(\mu) > m_i(\lambda)\} = \#\{m_i(\mu) < m_i(\lambda)\} + 1$ and $\tilde{\mathcal{T}}_0(x) = x$, (2.4.1) still holds. See Example 2.2 and 2.3 for an illustration.

Example 2.2. Consider $\lambda = (6, 5, 4, 4, 1)$ and $\mu = (6, 6, 4, 4, 3)$ with $\ell(\lambda) = \ell(\mu)$, we can check that

$$\left(\begin{array}{c} x \rightarrow 0 \\ \vdots \\ \dots -6 \quad -5 \quad -4 \quad -3 \quad -2 \quad -1 \\ \vdots \end{array} \begin{array}{c} |\lambda\rangle \\ \uparrow \uparrow \uparrow \\ |\mu\rangle \end{array} \rightarrow 0 \right) = \left(\begin{array}{c} x \rightarrow 0 \\ \vdots \\ \dots 0 \quad 1 \quad 2 \quad 3 \quad 4 \quad 5 \quad 6 \quad \dots \\ \vdots \end{array} \begin{array}{c} |\lambda\rangle \\ \downarrow \downarrow \downarrow \\ |\mu\rangle \end{array} \rightarrow 0 \right)$$

Example 2.3. Consider $\lambda = (6, 5, 4, 4, 1)$ and $\mu = (6, 6, 4, 4, 3, 1)$ with $\ell(\mu) = \ell(\lambda) + 1$, we can check

$$\left(\begin{array}{c} x \rightarrow 0 \\ \vdots \\ \dots -6 \quad -5 \quad -4 \quad -3 \quad -2 \quad -1 \\ \vdots \end{array} \begin{array}{c} |\lambda\rangle \\ \uparrow \uparrow \uparrow \\ |\mu\rangle \end{array} \rightarrow 1 \right) = \left(\begin{array}{c} x \rightarrow 0 \\ \vdots \\ \dots 0 \quad 1 \quad 2 \quad 3 \quad 4 \quad 5 \quad 6 \quad \dots \\ \vdots \end{array} \begin{array}{c} |\lambda\rangle \\ \downarrow \downarrow \downarrow \\ |\mu\rangle \end{array} \rightarrow 0 \right)$$

As a corollary, we can get the equivalence of two definitions of non-skew *ssHL functions* and their dual. In fact, we can also prove the equivalence of two definitions of non-skew *ssHL functions* and their dual directly by calculating the symmetrization formulas of f_μ and g_μ . We just sketch the computing method of the first definition, the result of the second definition can be found in [Bor17], [BP16], [BP18], [BW20],[BMP19].

Note that the right boundary conditions in the definition of f_μ and g_μ (see Figure 4) are free. It is difficult for us to analyse this kind of boundary condition directly, so our first step is to transform the free boundary problem into a fixed boundary problem, where the paths on the most right horizontal edges have the same number. With this transformation, we can find

that the left and the right boundary are invariant under the action of F matrices. And with using the F matrices, we can define the twisted symmetric column operators. The next step is to represent the partition functions by the twisted column operators and write the explicit formulae of these operators. The last step is the calculation of a special configuration by the explicit formulae of the twisted column operators, and getting the symmetrization formulas of f_μ and g_μ by the symmetry. We refer to [WZJ16] for the details. Our computational process is just similar to section 3.2 in [WZJ16], so we omit it. At the end of this section, we just present the first step, which is convenient for us to derive the refined Cauchy identity and refined Littlewood identity in section 3.4 and section 3.5.

We consider the higher spin six vertex model on a larger domain $\mathbb{Z}_{\leq 0} \times \mathbb{Z}_{\leq -1}$. The global physical space now is: $V_0 \otimes V_1 \otimes V_2 \otimes \dots$, where each V_i for $i \geq 0$ is a copy of local vector space V , and the index number i is assigned to the vertical line with the abscissa $-i$. We still consider the global vector with finitely many nonzero local vectors, and this time the linear basis becomes:

$$(2.4.3) \quad |\lambda; K_0\rangle := |K_0\rangle_0 \otimes |\lambda\rangle = \bigotimes_{i=0}^{\infty} |K_i\rangle_i, \quad K_0 \in \mathbb{Z}_{\geq 0}, \quad |\lambda\rangle \in \mathbb{V}.$$

where $\lambda = 1^{K_1} 2^{K_2} \dots$, and the dual linear basis is similar:

$$(2.4.4) \quad \langle \mu; I_0 | := \langle I_0 |_0 \otimes \langle \mu | = \bigotimes_{k=0}^{\infty} \langle I_k |_k, \quad I_0 \in \mathbb{Z}_{\geq 0}, \quad \langle \lambda | \in \mathbb{V}^*.$$

where $\mu = 1^{I_1} 2^{I_2} \dots$.

In this way, the operators (2.2.3) and (2.2.4) can be extended to the following operators:

$$(2.4.5) \quad \bar{\mathcal{T}}(x) : \bigotimes_{i=0}^{\infty} |K_i\rangle_i \mapsto \sum_{I_0, I_1, I_2, \dots \in \mathbb{Z}_{\geq 0}} \left(x \rightarrow 0 \begin{array}{ccccccc} \dots & \dots & K_3 & K_2 & K_1 & & K_0 \\ \uparrow & \uparrow & \uparrow & \uparrow & \uparrow & & \uparrow \\ \dots & \dots & I_3 & I_2 & I_1 & & I_0 \end{array} \rightarrow 1 \right) \bigotimes_{i=0}^{\infty} |I_i\rangle_i,$$

$$(2.4.6) \quad \bar{\mathcal{T}}^*(x) : \bigotimes_{i=0}^{\infty} |K_i\rangle_i \mapsto \sum_{I_0, I_1, I_2, \dots \in \mathbb{Z}_{\geq 0}} \left(x \rightarrow 1 \begin{array}{ccccccc} \dots & \dots & K_3 & K_2 & K_1 & & K_0 \\ \uparrow & \uparrow & \uparrow & \uparrow & \uparrow & & \uparrow \\ \dots & \dots & I_3 & I_2 & I_1 & & I_0 \end{array} \rightarrow 0 \right) \bigotimes_{i=0}^{\infty} |I_i\rangle_i.$$

where the vertices in column 0 has the weights in Figure 6 and 7, which are the $s = 0$ case of vertex weights in Figure 1 and 2. The vertices in column $i \geq 1$ is the same as in operator (2.2.3) and (2.2.4).

The choice of the specific weights in the column 0 enable us to give the non-skew *ssHL functions* $f_\mu(x_1, \dots, x_n)$ and $g_\mu(x_1, \dots, x_n)$ the alternative expressions:

$$(2.4.7) \quad \prod_{i=1}^n x_i f_\mu(x_1, \dots, x_n) = \langle \mu; n - \ell | \bar{\mathcal{T}}(x_n) \dots \bar{\mathcal{T}}(x_1) | \emptyset; 0 \rangle$$

$$(2.4.8) \quad \prod_{j=1}^{n-\ell} (1 - q^j) \prod_{i=1}^n x_i g_\mu(x_1, \dots, x_n) = \langle \emptyset; 0 | \bar{\mathcal{T}}^*(x_1) \dots \bar{\mathcal{T}}^*(x_n) | \mu; n - \ell \rangle$$

$L_{x,0}(I, j; K, \ell)$	1	x	$1 - q^{I+1}$	x

FIGURE 6. Type 1 vertex with $s = 0$.

$M_{x,0}(I, j; K, \ell)$	x	1	$x(1 - q^{I+1})$	1

FIGURE 7. Type 2 vertex with $s = 0$.

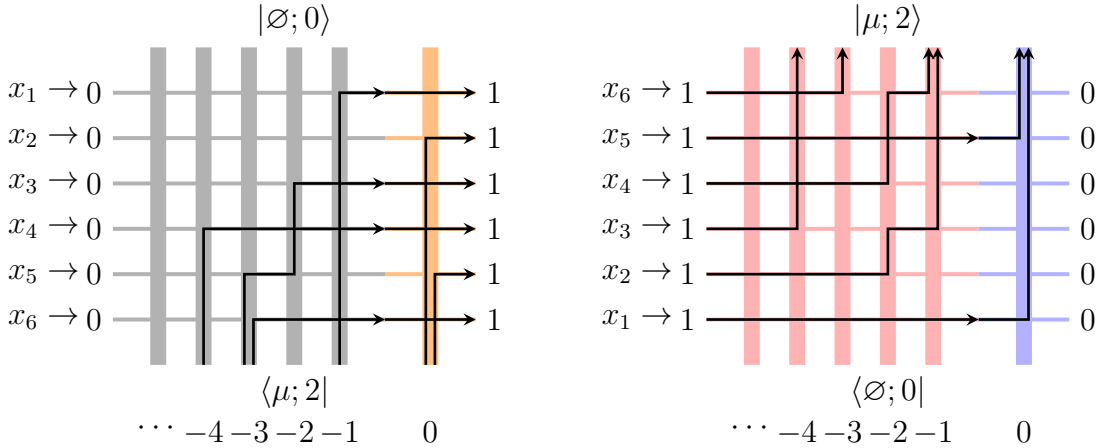


FIGURE 8. Left panel: a configuration of $x_1 \cdots x_6 f_\mu(x_1, \dots, x_6)$ with $\mu = (4, 3, 3, 1)$. Right panel: a configuration of $(1-q)(1-q^2)x_1 \cdots x_6 g_\mu(x_1, \dots, x_6)$ with $\mu = (4, 3, 1, 1)$.

The typical configurations in the partition functions are given in Figure 8.

3. COMBINATORIAL IDENTITIES FROM INTEGRABILITY

In this section, we use the first definition in section 2.2 to derive a series of combinatorial identities from the integrability of the higher spin six vertex model. Section 3.1 introduces the stochastic R-vertex and their Boltzmann weights, together with the vertex 1 and 2, we can get the intertwining equation by direct check. Section 3.2 and 3.3 give the skew Cauchy identity and skew Littlewood identity. The refined Cauchy identity and refined Littlewood identity are given in section 3.4 and 3.5.

3.1. Integrability of the higher spin six vertex model. Integrability of the higher spin six vertex model with vertex 1 and 2 is given by the intertwining equation:

(3.1.1)

$$\sum_{0 \leq k_1, k_3 \leq 1} \sum_{K \in \mathbb{Z}_{\geq 0}} \begin{array}{c} \begin{array}{c} i_1 \nearrow \\ i_3 \searrow \end{array} \\ \begin{array}{c} k_3 \rightarrow \\ k_1 \rightarrow \end{array} \\ \begin{array}{c} j_3 \rightarrow \\ j_1 \rightarrow \end{array} \\ \begin{array}{c} \nearrow x \\ \searrow y \end{array} \end{array} = \sum_{0 \leq k_1, k_3 \leq 1} \sum_{K \in \mathbb{Z}_{\geq 0}} \begin{array}{c} \begin{array}{c} y \nwarrow \\ x \nwarrow \end{array} \\ \begin{array}{c} i_1 \rightarrow \\ i_3 \rightarrow \end{array} \\ \begin{array}{c} k_1 \rightarrow \\ k_3 \rightarrow \end{array} \\ \begin{array}{c} \nearrow j_3 \\ \searrow j_1 \end{array} \\ \begin{array}{c} \nearrow x \\ \searrow y \end{array} \end{array}$$

where the rotated vertices is the R -vertex, and we list their Boltzmann weights in Figure 9. For any fixed $i, j \in \{0, 1\}$, the R -vertex satisfy the stochastic property:

(3.1.2)
$$\sum_{0 \leq k \leq 1} \sum_{0 \leq \ell \leq 1} \begin{array}{c} j \nearrow k \\ i \searrow \ell \end{array} = 1.$$

$\begin{array}{c} j \nearrow k \\ i \searrow \ell \end{array}$	$\begin{array}{c} 0 \nearrow 0 \\ 0 \searrow 0 \end{array}$	$\begin{array}{c} 0 \nearrow 1 \\ 1 \searrow 0 \end{array}$	$\begin{array}{c} 0 \nearrow 0 \\ 1 \searrow 1 \end{array}$	$\begin{array}{c} 1 \nearrow 1 \\ 1 \searrow 1 \end{array}$	$\begin{array}{c} 1 \nearrow 0 \\ 0 \searrow 1 \end{array}$	$\begin{array}{c} 1 \nearrow 1 \\ 0 \searrow 0 \end{array}$
$R(i, j; k, \ell)$	1	$\frac{q(1-xy)}{1-qxy}$	$\frac{1-q}{1-qxy}$	1	$\frac{1-xy}{1-qxy}$	$\frac{(1-q)xy}{1-qxy}$

FIGURE 9. Boltzmann weight for R -vertex in (3.1.1)

3.2. Skew Cauchy identity. The skew Cauchy identity for $ssHL$ functions and their dual have been deduced in [BW20] by an algebraic method, we now give a combinatorial proof.

Theorem 3.1. Let x_1, \dots, x_m and y_1, \dots, y_n be complex numbers, such that

(3.2.1)
$$(x_i - s)(y_j - s) < (1 - sx_i)(1 - sy_j),$$

for any given $i = 1, \dots, m$ and $j = 1, \dots, n$. For the fixed two partitions λ and μ , the skew $ssHL$ functions (2.2.7) and their dual (2.2.8) satisfy the skew Cauchy identity:

(3.2.2)
$$\prod_{i=1}^m \prod_{j=1}^n \frac{1 - x_i y_j}{1 - q x_i y_j} \sum_{\kappa} g_{\kappa/\lambda}(y_1, \dots, y_n) f_{\kappa/\mu}(x_1, \dots, x_m) = \sum_{\nu} f_{\lambda/\nu}(x_1, \dots, x_m) g_{\mu/\nu}(y_1, \dots, y_n)$$

Proof. Following the definition (2.2.7) and (2.2.8), the left-hand side of 3.2.2 can be expressed by a summation of partition functions in the higher spin six vertex model:

$$(3.2.3) \quad \sum_{0 \leq s_1, \dots, s_n \leq 1} \sum_{0 \leq s'_1, \dots, s'_m \leq 1}$$

$\cdots -4 -3 -2 -1$

where the left edge is glued with a $m \times n$ lattice of R -vertex in Figure 9. From the condition (3.2.1), we know that, there are no paths to come into the domain from the top m rows, and while there is one path to go into the domain from any bottom n rows. By reusing the intertwining equation (3.1.1), we can turn (3.2.3) into the following summation:

$$(3.2.4) \quad \sum_{0 \leq s_1, \dots, s_n \leq 1} \sum_{0 \leq s'_1, \dots, s'_m \leq 1}$$

$\cdots -4 -3 -2 -1$

(3.2.4) can be factorized into two parts:

(3.2.5)

$$\sum_{0 \leq t_1, \dots, t_n \leq 1} \sum_{0 \leq t'_1, \dots, t'_m \leq 1} \begin{array}{c} \text{\scriptsize } |\mu\rangle \\ \begin{array}{ccc} y_n \rightarrow 1 & \xrightarrow{\text{red}} & t_n \\ \vdots \rightarrow 1 & \xrightarrow{\text{red}} & \vdots \\ y_1 \rightarrow 1 & \xrightarrow{\text{red}} & t_1 \\ x_1 \rightarrow 0 & \xrightarrow{\text{grey}} & t'_1 \\ \vdots \rightarrow 0 & \xrightarrow{\text{grey}} & \vdots \\ x_m \rightarrow 0 & \xrightarrow{\text{grey}} & t'_m \end{array} \\ \text{\scriptsize } \langle \lambda | \\ \cdots -4 -3 -2 -1 \end{array} \times \sum_{0 \leq s_1, \dots, s_n \leq 1} \sum_{0 \leq s'_1, \dots, s'_m \leq 1} \begin{array}{ccc} t_n & \xrightarrow{\text{grey}} & s'_1 \cdots s'_m \\ \vdots & \xrightarrow{\text{grey}} & \vdots \\ t_1 & \xrightarrow{\text{grey}} & s_n \\ t'_1 & \xrightarrow{\text{grey}} & s_1 \\ \vdots & \xrightarrow{\text{grey}} & \vdots \\ t'_m & \xrightarrow{\text{grey}} & \vdots \end{array}$$

Following the stochastic property (3.1.2), we can find that

$$(3.2.6) \quad \sum_{0 \leq s_1, \dots, s_n \leq 1} \sum_{0 \leq s'_1, \dots, s'_m \leq 1} \begin{array}{ccc} t_n & \xrightarrow{\text{grey}} & s'_1 \cdots s'_m \\ \vdots & \xrightarrow{\text{grey}} & \vdots \\ t_1 & \xrightarrow{\text{grey}} & s_n \\ t'_1 & \xrightarrow{\text{grey}} & s_1 \\ \vdots & \xrightarrow{\text{grey}} & \vdots \\ t'_m & \xrightarrow{\text{grey}} & \vdots \end{array} = 1$$

for fix t_1, \dots, t_n and t'_1, \dots, t'_m . The remaining part of (3.2.5) is just equal to the right-hand side of (3.2.2). \square

Corollary 3.2. *Let x_1, \dots, x_m and y_1, \dots, y_n be complex numbers satisfy (3.2.1) for all $i = 1, \dots, m$ and $j = 1, \dots, n$, the non-skew ssHL functions (2.2.9) and their dual (2.2.10) satisfy the Cauchy identity:*

$$(3.2.7) \quad \prod_{i=1}^m \prod_{j=1}^n \frac{1 - x_i y_j}{1 - q x_i y_j} \sum_{\kappa} g_{\kappa}(y_1, \dots, y_n) f_{\kappa}(x_1, \dots, x_m) = 1.$$

Remark 3.3. *Using a similar method, we can make a connection between the stochastic six vertex model and the (stable) spin Hall-Littlewood process just like the way in [BBW16], we refer to it for details.*

3.3. Skew Littlewood identity. Comparing with the skew Cauchy identity, the skew Littlewood identity need more work. In addition to the intertwining equation (3.1.1), we also need the reflection equation:

Proposition 3.4. Let $K \geq 0$ be any non-negative integer, and fix $j, k \in \{0, 1\}$. The following identity holds:

$$(3.3.1) \quad \sum_{I=0}^{\infty} \prod_{k=1}^I \frac{1 - q^{2k-1}}{1 - s^2 q^{2k-1}} \left(\begin{array}{c} \xrightarrow{j} \bullet \xrightarrow{\quad} \ell \\ \uparrow K \\ \text{---} \\ \downarrow 2I \end{array} \right) = \sum_{I=0}^{\infty} \prod_{k=1}^I \frac{1 - q^{2k-1}}{1 - s^2 q^{2k-1}} \left(\begin{array}{c} \xrightarrow{j} \bullet \xrightarrow{\quad} \ell \\ \uparrow K \\ \text{---} \\ \downarrow 2I \end{array} \right)$$

where the dot turn the state $0 \leq i \leq 1$ into state $1 - i$.

Proof. This is a generalization of [BBCW18, Proposition 4.9] in the higher spin case, and the proof is similar. \square

Theorem 3.5. Let x_1, \dots, x_n be complex numbers such that x_i, x_j satisfy the condition (3.2.1) for any given $1 \leq i < j \leq n$. For any fixed partition μ , the skew ssHL functions (2.2.7) and their dual (2.2.8) satisfy the skew Littlewood identity:

$$(3.3.2) \quad \sum_{\lambda' \text{ even}} b_{\lambda}^{el} f_{\lambda/\mu}(x_1, \dots, x_n) = \prod_{1 \leq i < j \leq n} \frac{1 - qx_i x_j}{1 - x_i x_j} \sum_{\nu' \text{ even}} b_{\nu}^{el} g_{\mu/\nu}(x_1, \dots, x_n)$$

where the summation is over all the partitions such that their conjugate is even, and the coefficient b_{μ}^{el} is given by

$$(3.3.3) \quad b_{\mu}^{el} = \prod_{i=1}^{\infty} \prod_{k=1}^{m_i(\mu)/2} \frac{1 - q^{2k-1}}{1 - s^2 q^{2k-1}}.$$

Proof. We start by expressing the left-hand side of (3.3.2) as a summation of partition functions in the higher spin six vertex model:

$$(3.3.4) \quad \sum_{0 \leq s_1, \dots, s_n \leq 1} \sum_{\lambda' \text{ even}} b_{\lambda}^{el} \begin{array}{c} \begin{array}{c} \xrightarrow{x_1 \rightarrow 0} \uparrow \uparrow \uparrow \uparrow \uparrow \rightarrow s_1 \\ \vdots \rightarrow 0 \\ \vdots \\ \xrightarrow{x_{n-1} \rightarrow 0} \uparrow \uparrow \uparrow \uparrow \uparrow \rightarrow s_{n-1} \\ \vdots \\ \xrightarrow{x_n \rightarrow 0} \uparrow \uparrow \uparrow \uparrow \uparrow \rightarrow s_n \end{array} \\ \langle \lambda | \\ \cdots -4 -3 -2 -1 \end{array}$$

Employing the reflection equation (3.3.1), we can turn the L vertex in the bottom into the M vertex:

$$(3.3.5) \quad \prod_{i=1}^{n-1} \frac{1 - qx_i x_n}{1 - x_i x_n} \sum_{0 \leq s_1, \dots, s_n \leq 1} \sum_{\lambda' \text{ even}} b_\lambda^{el} \begin{array}{c} \begin{array}{c} | \mu \rangle \\ \uparrow \uparrow \uparrow \uparrow \uparrow \\ \text{---} s_1 \leftarrow x_1 \\ \vdots \\ \text{---} s_{n-1} \leftarrow x_{n-1} \\ \text{---} s_n \leftarrow x_n \\ \bullet \end{array} \\ \begin{array}{c} \text{---} 1 \\ \text{---} 0 \\ \text{---} 0 \\ \text{---} 0 \end{array} \end{array}$$

where we have introduced $(n - 1)$ R-vertex at the left edge so that we can perform the intertwining equation (3.1.1):

$$(3.3.6) \quad \prod_{i=1}^{n-1} \frac{1 - qx_i x_n}{1 - x_i x_n} \sum_{0 \leq s_1, \dots, s_n \leq 1} \sum_{\lambda' \text{ even}} b_\lambda^{el} \begin{array}{c} \begin{array}{c} | \mu \rangle \\ \uparrow \uparrow \uparrow \uparrow \uparrow \\ \text{---} s_1 \leftarrow x_1 \\ \vdots \\ \text{---} s_{n-1} \leftarrow x_{n-1} \\ \text{---} s_n \leftarrow x_n \\ \bullet \end{array} \\ \begin{array}{c} x_n \rightarrow 1 \\ x_1 \rightarrow 0 \\ \vdots \rightarrow 0 \\ x_{n-1} \rightarrow 0 \end{array} \end{array}$$

Integrating the above procedure, we can obtain the following expression:

$$(3.3.7) \quad \prod_{1 \leq i < j \leq N} \frac{1 - qx_i x_j}{1 - x_i x_j} \sum_{0 \leq s_1, \dots, s_n \leq 1} \sum_{\lambda' \text{ even}} b_\lambda^{el} \begin{array}{c} \begin{array}{c} | \mu \rangle \\ \uparrow \uparrow \uparrow \uparrow \uparrow \\ \text{---} s_1 \leftarrow x_1 \\ \vdots \\ \text{---} s_{n-1} \leftarrow x_{n-1} \\ \text{---} s_n \leftarrow x_n \\ \bullet \end{array} \\ \begin{array}{c} x_n \rightarrow 1 \\ x_{n-1} \rightarrow 1 \\ \vdots \rightarrow 1 \\ x_1 \rightarrow 1 \end{array} \end{array}$$

The above summation can be factorized into two parts:

(3.3.8)

$$\sum_{0 \leq t_1, \dots, t_n \leq 1} \sum_{\lambda' \text{ even}} b_\lambda^{el} \begin{array}{c} | \mu \rangle \\ \begin{array}{c} x_n \rightarrow 1 \\ \vdots \rightarrow 1 \\ \vdots \rightarrow 1 \\ x_1 \rightarrow 1 \end{array} \begin{array}{c} \uparrow \\ \uparrow \\ \uparrow \\ \uparrow \\ \uparrow \end{array} \begin{array}{c} t_n \\ \vdots \\ t_1 \end{array} \\ \langle \nu | \\ \cdots -4 -3 -2 -1 \end{array} \times \sum_{0 \leq s_1, \dots, s_n \leq 1} \begin{array}{c} t_n \\ \vdots \\ t_1 \end{array} \begin{array}{c} \swarrow \\ \swarrow \\ \swarrow \\ \swarrow \\ \swarrow \end{array} \begin{array}{c} s_1 \\ \vdots \\ s_n \end{array}$$

Following the stochastic property (3.1.2), we can find that

$$(3.3.9) \quad \sum_{0 \leq s_1, \dots, s_n \leq 1} \begin{array}{c} t_n \\ \vdots \\ t_1 \end{array} \begin{array}{c} \swarrow \\ \swarrow \\ \swarrow \\ \swarrow \\ \swarrow \end{array} \begin{array}{c} s_1 \\ \vdots \\ s_n \end{array} = 1$$

for fix t_1, \dots, t_n . The remaining part of (3.3.8) is just equal to the right-hand side of (3.3.2). \square

Corollary 3.6. *Let x_1, \dots, x_n be complex numbers such that x_i, x_j satisfy the condition (3.2.1) for all $1 \leq i < j \leq n$, the non-skew ssHL functions (2.2.9) and their dual (2.2.10) satisfy the Littlewood identity:*

$$(3.3.10) \quad \sum_{\lambda' \text{ even}} b_\lambda^{el} f_\lambda(x_1, \dots, x_n) = \prod_{1 \leq i < j \leq n} \frac{1 - qx_i x_j}{1 - x_i x_j}$$

where the summation is over all the partitions such that their conjugate is even, and the coefficient b_μ^{el} is given by (3.3.3).

Remark 3.7. *Using a similar method, we can make a bridge between the stochastic six vertex model in a half-quadrant and the half-space (stable) spin Hall-Littlewood process just like the way in [BBCW18]. But we are not going to repeat that process here. Instead, we give another approach to relate a new half-space stochastic six vertex model to the half-space (stable) spin Hall-Littlewood process in section 4.*

3.4. Refined Cauchy identity. The expressions of *ssHL functions* and their dual in 2.4.7 and 2.4.8 admit us to derive the refined version of Cauchy identity (3.2.7):

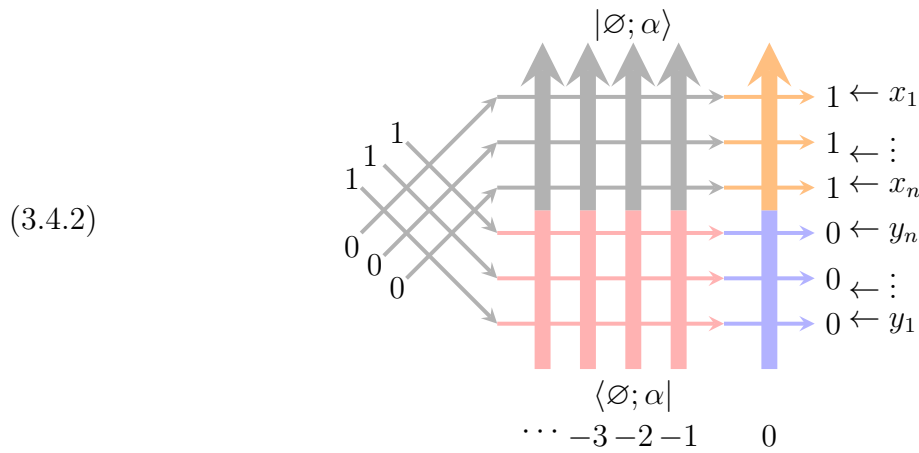
Theorem 3.8. *The non-skew ssHL functions and their dual satisfy the following refined Cauchy identity:*

$$(3.4.1) \quad \sum_{\lambda} \prod_{i=1}^{m_0(\lambda)} (1 - uq^i) f_\lambda(x_1, \dots, x_n; q, s) g_\lambda(y_1, \dots, y_n; q, s)$$

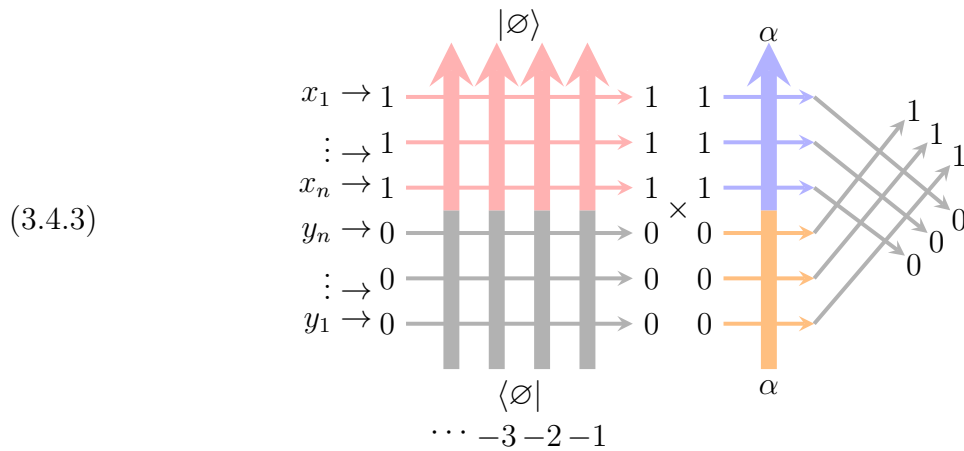
$$= \frac{\prod_{i,j=1}^n (1 - qx_i y_j)}{\prod_{1 \leq i < j \leq n} (x_i - x_j)(y_i - y_j)} \det_{1 \leq i, j \leq n} \left[\frac{1 - uq + (u - 1)qx_i y_j}{(1 - x_i y_j)(1 - qx_i y_j)} \right],$$

where $u = q^\alpha$ can be extended to an arbitrary parameter, $m_0(\lambda) = n - \ell(\lambda)$.

Proof. The proof is in the same vein as the procedure in the proof of Theorem 3.1. This time, however, we use the intertwining equation (3.1.1) to transform the partition function



into the following partition functions



where the Boltzmann weight of the left part is 1, and the Boltzmann weight of the right part is

(3.4.4)

$$= \frac{\prod_{i=1}^n (x_i y_i) \prod_{i,j=1}^n (1 - x_i y_j)}{\prod_{1 \leq i < j \leq n} (x_i - x_j)(y_i - y_j)} \det_{1 \leq i, j \leq n} \left[\frac{1 - uq + (u - 1)qx_i y_j}{(1 - x_i y_j)(1 - qx_i y_j)} \right],$$

which can be derived just like the lemma 5 in [WZJ16]. □

Remark 3.9. *The result in (3.4.1) is a one-parameter generalization of the refined Cauchy identity for Hall-Littlewood polynomials in [WZJ16]. Moreover, (3.4.1) is a degenerated case of the refined Cauchy identity for the (non-stable) inhomogeneous spin Hall-Littlewood polynomials in a recent work [Pet20], with $s_0 = 0$, $s_x = s$, $\xi_x = 1$ and the relations [Pet20, (2.12),(2.14)] between the stable/non-stable spin Hall-Littlewood polynomials.*

3.5. Refined Littlewood identity. The expressions of *ssHL functions*, as well as their dual in 2.4.7 and 2.4.8 admit us to derive the refined version of Littlewood identity (3.3.10):

Theorem 3.10. *The non-skew ssHL functions and their dual satisfy the following refined Littlewood identity:*

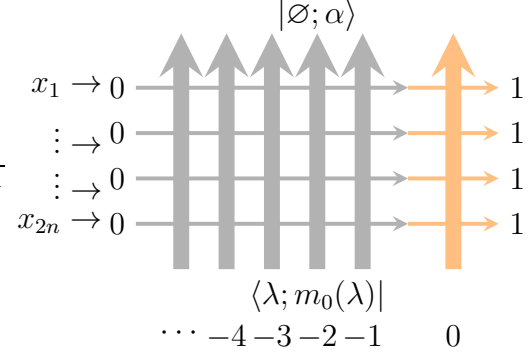
$$(3.5.1) \quad \sum_{\lambda: m_i(\lambda) \text{ even}} \prod_{k=1}^{m_0(\lambda)/2} (1 - uq^{2k-1}) \prod_{i=1}^{\infty} \prod_{j=1}^{m_i(\lambda)/2} \frac{1 - q^{2j-1}}{1 - s^2 q^{2j-1}} f_{\lambda}(x_1, \dots, x_{2n}; q, s) = \prod_{1 \leq i < j \leq 2n} \left(\frac{1 - qx_i x_j}{x_i - x_j} \right) \text{Pf}_{1 \leq i < j \leq 2n} \left[\frac{(x_i - x_j)(1 - uq + (u - 1)qx_i x_j)}{(1 - x_i x_j)(1 - qx_i x_j)} \right],$$

where $u = q^{\alpha}$ can be extended to an arbitrary parameter, $m_0(\lambda) = 2n - \ell(\lambda)$.

Proof. The proof is in the same vein as the procedure in [WZJ16, Section 5]. Here, but we use the intertwining equation (3.1.1) and the reflection equation (3.3.1) to transform the

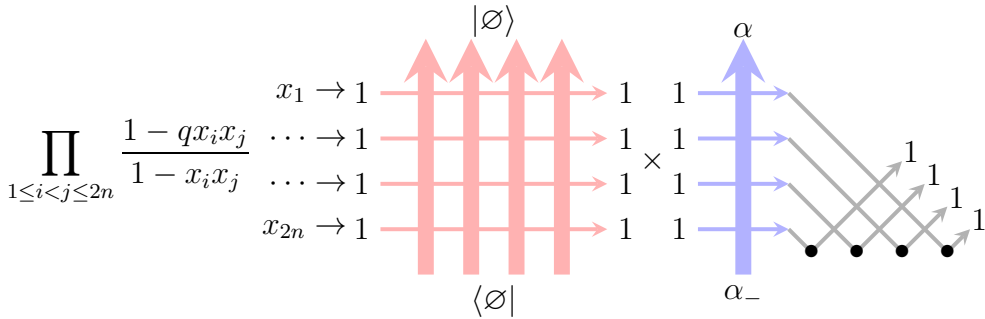
partition function

(3.5.2)

$$\sum_{\lambda: m_i(\lambda) \text{ even}} \prod_{k=1}^{m_0(\lambda)/2} (1 - uq^{2k-1}) \prod_{i=1}^{\infty} \prod_{j=1}^{m_i(\lambda)/2} \frac{1 - q^{2j-1}}{1 - s^2 q^{2j-1}}$$


The diagram shows a grid of horizontal lines representing variables $x_1 \rightarrow 0, \dots, x_{2n} \rightarrow 0$ on the left and 1 on the right. Vertical arrows represent the partition $\langle \emptyset; \alpha \rangle$ at the top and $\langle \lambda; m_0(\lambda) \rangle$ at the bottom. The bottom labels are $\dots -4 -3 -2 -1 \quad 0$. The arrows are grey, except for one orange arrow on the right.

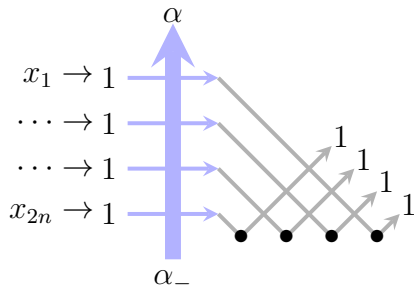
into the following partition functions

$$(3.5.3) \quad \prod_{1 \leq i < j \leq 2n} \frac{1 - qx_i x_j}{1 - x_i x_j}$$


The diagram shows a grid of horizontal lines with variables $x_1 \rightarrow 1, \dots, x_{2n} \rightarrow 1$ on the left and 1 on the right. Red vertical arrows represent $\langle \emptyset \rangle$ and a blue vertical arrow represents α . Grey lines with dots at the bottom represent α_- . The diagram is labeled with $\langle \emptyset |$ and α_- .

where the Boltzmann weight of the left part is 1. Similar with lemma 7 in [WZJ16], we can get that

(3.5.4)



$$= \left(\prod_{i=1}^{2n} x_i \right) \text{Pf}_{1 \leq i < j \leq 2n} \left[\frac{(x_i - x_j)(1 - uq + (u - 1)qx_i x_j)}{(1 - x_i x_j)(1 - qx_i x_j)} \right]$$

□

Remark 3.11. *The result in (3.5.1) is a one-parameter generalization of refined Littlewood identity for Hall-Littlewood polynomials in [WZJ16]. Moreover, (3.5.1) is also a degenerated case of the refined Littlewood identity for the (non-stable) inhomogeneous spin Hall-Littlewood polynomials in recent work [Gav21], with $s_0 = 0$, $s_x = s$, $\xi_x = 1$ and the relations [Pet20, (2.12),(2.14)] between the stable/non-stable spin Hall-Littlewood polynomials.*

Although the (non-stable) inhomogeneous spin Hall-Littlewood polynomials have similar properties: such as skew Cauchy identity, refined Cauchy identity and refined Littlewood identity, but they don't admit the skew Littlewood identity. Skew Littlewood identity is the

key to lift the full-space Yang-Baxter random field in [BMP19] to a half-space version, see section 4 for details.

4. HALF-SPACE RANDOM FIELD

In this section, we use the second definition in section 2.3 to construct a stochastic object, which we call the half-space Yang-Baxter field. Section 4.1 introduces the skew Cauchy-Littlewood structure for the *ssHL functions*. Section 4.2 introduces the half-space Yang-Baxter random field. We sample the half-space random field via the Markov transition operators in section 4.3, and construct the transition operators in section 4.4 and section 4.5. The evolution of the lengths of the partitions in the half-space Yang-Baxter field are introduced in section 4.6. Section 4.7 introduce a dynamic version of stochastic six vertex model in a half-quadrant and a dynamic version of discrete-time interacting particle system.

4.1. Skew Cauchy-Littlewood structure. We use the *skew Cauchy-Littlewood structure* to overview the properties of *ssHL functions* and their dual:

- (1) Symmetry: $f_{\lambda/\mu}, g_{\lambda/\mu}$ are symmetric rational functions.
- (2) Interlacing condition: for all $\mu, \lambda \in \mathbb{Y}$ we have

$$(4.1.1) \quad f_{\lambda/\mu}(x) \neq 0 \quad \text{iff} \quad \mu \prec \lambda; \quad g_{\lambda/\mu}(y) \neq 0 \quad \text{iff} \quad \mu \prec \lambda.$$

- (3) Branching rule: for all $\nu, \lambda \in \mathbb{Y}$ we have

$$(4.1.2) \quad f_{\lambda/\nu}(x, y) = \sum_{\mu} f_{\lambda/\mu}(x) f_{\mu/\nu}(y), \quad g_{\lambda/\nu}(x, y) = \sum_{\mu} g_{\lambda/\mu}(x) g_{\mu/\nu}(y).$$

- (4) Skew Cauchy identity: for all $\mu, \lambda \in \mathbb{Y}$ and the rational function $\Pi(x; y) = \frac{1-qty}{1-xy}$, we have

$$(4.1.3) \quad \Pi(x; y) \sum_{\varkappa} f_{\mu/\varkappa}(x) g_{\lambda/\varkappa}(y) = \sum_{\nu} f_{\nu/\lambda}(x) g_{\nu/\mu}(y)$$

holds for all $(x, y) \in \text{Adm} = \{(x, y) \in \mathbb{C}^2 : (x-s)(y-s) < (1-sx)(1-sy)\}$.

- (5) Skew Littlewood identity: for any $\varkappa \in \mathbb{Y}$ we have

$$(4.1.4) \quad \sum_{\tau' \text{ even}} b_{\tau}^{el} g_{\varkappa/\tau}(x) = \sum_{\mu' \text{ even}} b_{\lambda}^{el} f_{\lambda/\varkappa}(x)$$

where $b_{\mu}^{el} = \prod_{i=1}^{\infty} \prod_{k=1}^{m_i(\mu)/2} \frac{1-q^{2k-1}}{1-s^2q^{2k-1}}$. Note that there are unique τ and λ such that τ' and λ' are even and $\tau \prec \varkappa \prec \lambda$, so the sum reduce to only one term in each side.

- (6) Nonnegativity: With the assumption of the external parameters $q \in (0, 1)$, $s \in (-1, 0)$, $f_{\lambda/\mu}(x)$ and $g_{\lambda/\mu}(y)$ are non-negative for any $x, y \in [0, 1)$ and any $\lambda, \mu \in \mathbb{Y}$.

Comparing with the skew Cauchy structure introduced in [BMP19], we have one more identity, the skew Littlewood identity (4.1.4), which is the single variable version of (3.3.2). See Example 4.1 for an illustration. We refer to [BW20, BMP19] for the proof of the skew Cauchy structure.

Example 4.1. We consider the case $\varkappa = (4, 4, 4, 3, 2, 2, 1)$, $\sum_{\tau' \text{ even}} b_{\tau}^{el} g_{\varkappa/\tau}(x)$ trivialize into only one term with $\tau = (4, 4, 3, 3, 2, 2)$:

$$\sum_{\tau' \text{ even}} b_{\tau}^{el} g_{\varkappa/\tau}(x)$$

$$\begin{aligned}
&= \frac{1-q}{1-s^2q} \cdot \frac{1-q}{1-s^2q} \cdot \frac{1-q}{1-s^2q} \left(x \rightarrow 0 \begin{array}{c} \infty \\ \uparrow \\ \uparrow \\ \uparrow \\ \uparrow \\ \uparrow \\ 0 \end{array} \begin{array}{c} |z\rangle \\ \uparrow \\ \uparrow \\ \uparrow \\ \uparrow \\ \uparrow \\ \uparrow \\ 0 \end{array} \begin{array}{c} \infty \\ \downarrow \\ \downarrow \\ \downarrow \\ \downarrow \\ \downarrow \\ \downarrow \\ 0 \end{array} \end{array} \right) \\
&= \frac{1-q}{1-s^2q} \cdot \frac{1-q}{1-s^2q} \cdot \frac{1-q}{1-s^2q} \cdot x \cdot \frac{1-q}{1-sx} \cdot \frac{1-sxq^2}{1-sx} \cdot \frac{x(1-s^2q)}{1-sx} \cdot \frac{1-q^3}{1-sx},
\end{aligned}$$

and $\sum_{\lambda' \text{ even}} b_{\lambda'}^{el} f_{\lambda'/z}(x)$ reduce to only one term with $\lambda = (4, 4, 4, 4, 2, 2, 1, 1)$:

$$\begin{aligned}
&\sum_{\lambda' \text{ even}} b_{\lambda'}^{el} f_{\lambda'/z}(x) \\
&= \frac{1-q}{1-s^2q} \cdot \frac{1-q}{1-s^2q} \cdot \left(\frac{1-q}{1-s^2q} \cdot \frac{1-q^3}{1-s^2q^3} \right) \left(x \rightarrow 0 \begin{array}{c} \infty \\ \downarrow \\ \downarrow \\ \downarrow \\ \downarrow \\ \downarrow \\ \downarrow \\ 0 \end{array} \begin{array}{c} |z\rangle \\ \downarrow \\ \downarrow \\ \downarrow \\ \downarrow \\ \downarrow \\ \downarrow \\ 0 \end{array} \begin{array}{c} \infty \\ \uparrow \\ \uparrow \\ \uparrow \\ \uparrow \\ \uparrow \\ \uparrow \\ 0 \end{array} \end{array} \right) \\
&= \frac{1-q}{1-s^2q} \cdot \frac{1-q}{1-s^2q} \cdot \left(\frac{1-q}{1-s^2q} \cdot \frac{1-q^3}{1-s^2q^3} \right) \cdot x \cdot \frac{1-s^2q}{1-sx} \cdot \frac{1-sxq^2}{1-sx} \cdot \frac{(1-q)x}{1-sx} \cdot \frac{1-s^2q^3}{1-sx},
\end{aligned}$$

One can find that (4.1.4) holds.

Further, we introduce the notation $\mathcal{G}_z(x)$:

$$(4.1.5) \quad \mathcal{G}_z(x) = \sum_{\tau' \text{ even}} b_{\tau'}^{el} g_{z/\tau}(x).$$

Now combining the skew Cauchy identity (4.1.3) and skew Littlewood identity (4.1.4), we obtain the generalized skew Littlewood identity:

$$(4.1.6) \quad \Pi(x; y) \sum_{\kappa} g_{\mu/\kappa}(x) \mathcal{G}_{\kappa}(y) = \sum_{\nu} f_{\nu/\mu}(y) \mathcal{G}_{\nu}(x).$$

4.2. Half-space Yang-Baxter random field. Consider the half-space $\mathbb{H} = \{(i, j) \in \mathbb{Z}^2 : 0 \leq i \leq j\}$. A *caudate zigzag path* on \mathbb{H} is a zigzag path with a tail, the zigzag path is an up-left path which grows on the integer grid:

$$(4.2.1) \quad \omega = \{\omega_k = (i_k, j_k), 0 \leq k \leq N, i_0 = j_0 = n, i_N = 0, \omega_{k+1} - \omega_k = \{-\mathbf{e}_1, \mathbf{e}_2\}\},$$

the tail $\{(i, i) \in \mathbb{R}^2, n-1 < i \leq n\}$ grows on the diagonal, where n and $N \in \mathbb{Z}_{\geq 0}$ depend on the zigzag path ω , and $\mathbf{e}_1, \mathbf{e}_2$ are the standard basis vectors $(1, 0), (0, 1)$. See an example of caudate zigzag path in Figure 10.

Definition 4.2. A family of random partitions $\boldsymbol{\lambda} = \{\lambda^{(i,j)} : (i, j) \in \mathbb{H}\}$ is called a half-space Yang-Baxter random field associated with the skew Cauchy-Littlewood structure of ssHL functions if:

- (1) The partitions satisfy $\lambda^{(i,j)} \prec \lambda^{(i,j+1)}$ and $\lambda^{(i,j)} \prec \lambda^{(i+1,j)}$ for all $(i, j) \in \mathbb{H}$.
- (2) Fix the partitions at the boundary $\lambda^{(0,j)} = \emptyset$ with the probability 1.

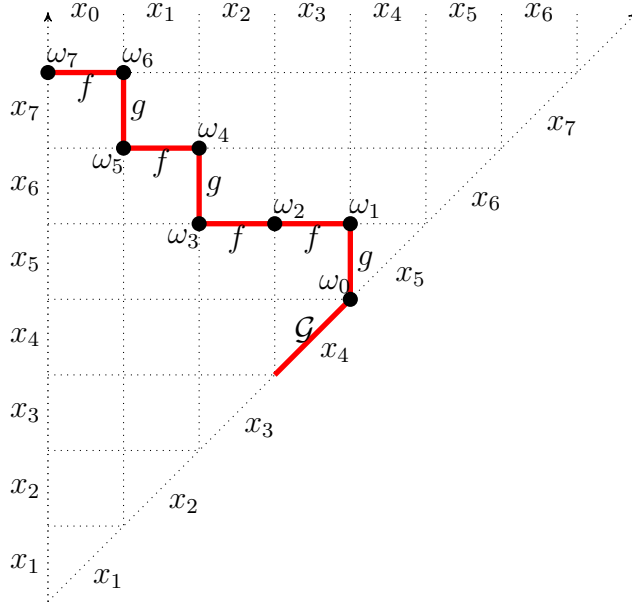


FIGURE 10. A caudate zigzag path in the half-quadrant \mathbb{H} .

(3) Assign the probability measure

$$(4.2.2) \quad \frac{1}{Z_\omega} \mathcal{G}_{\lambda^{\omega_0}}(x_n) \prod_{k \geq 1: \omega_{k+1} = \omega_k + \mathbf{e}_2} g_{\lambda^{\omega_{k+1}} / \lambda^{\omega_k}}(x_{j_{k+1}}) \prod_{\ell \geq 1: \omega_{\ell+1} = \omega_\ell - \mathbf{e}_1} f_{\lambda^{\omega_{\ell+1}} / \lambda^{\omega_\ell}}(x_{i_\ell})$$

to an event of finding partitions $\lambda^{\omega_0}, \dots, \lambda^{\omega_N}$ along a caudate zigzag path, and Z_ω is the normalization constant.

To visualize the half-space random field, we assign the specialization x_n to the diagonal boundary $(n-1, n-1) \rightarrow (n, n)$ for any given $n \geq 0$, as well as x_i to edges $(i, j) \rightarrow (i+1, j)$, and furthermore x_j to edges $(i, j-1) \rightarrow (i, j)$. For a caudate zigzag path ω , the probability of finding the sequence $\{\lambda^{\omega_k}, 0 \leq k \leq N\}$ is computed by climbing along ω . In the part of tail, one picks up $\mathcal{G}_{\lambda^{\omega_0}}(x_n)$ along the diagonal, for the zigzag path, one associates skew functions $g_{\lambda^{\omega_{k+1}} / \lambda^{\omega_k}}(x_{j_{k+1}})$ for certain k along the vertical edges, and skew functions $f_{\lambda^{\omega_{\ell+1}} / \lambda^{\omega_\ell}}(x_{i_\ell})$ for a given ℓ along the horizontal edges, respectively. See Figure 10 for an illustration. The normalization constant Z_ω can be calculated by two contraction principles in Figure 11. Similar contraction principles have been introduced in [BBCS18, BBC20], we recommend to readers for further reference.

The probability measure (4.2.2) is the analogue of the half-space Schur and Macdonald process defined in [BBCS18, BBC20], so we call it *half-space ssHL process*. The way we assign the specializations to the diagonal in the *half-space ssHL process* is different from the way in the half-space Macdonald case. In the half-space Macdonald process, the specialization on the diagonal remains intact as the random partitions evolve, while in the *half-space ssHL* case, the specialization on the diagonal is always changing. The change brings us a non-trivial dynamic way, which depends on the starting partitions. This is different from the push-block dynamics in [BBCS18, BBC20], we will further elaborate on this point in the following content.

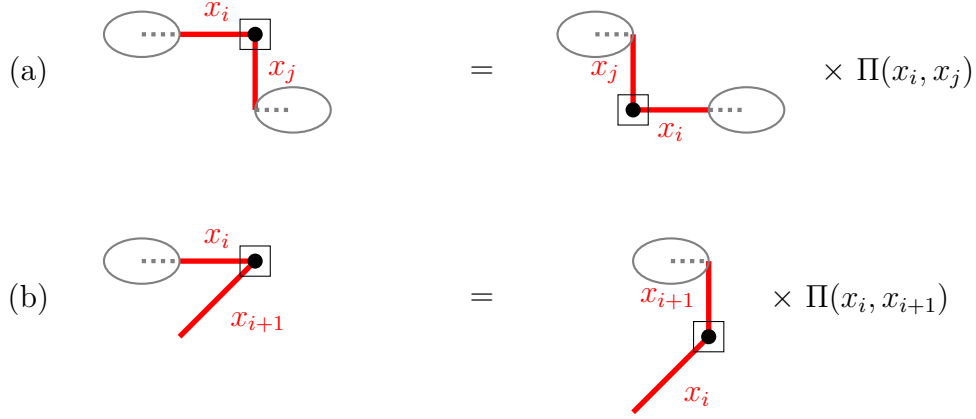


FIGURE 11. Graph (a) represents the skew Cauchy identity (4.1.3); Graph (b) represents the skew Littlewood identity (4.1.4). The boxes represent vertices whose partitions are being summed over; the edges are labelled by specializations; the blobs represent other terms which may arise in the weight of a path ω which are not involved in these identities.

4.3. Sampling a half-space random field via the Markov transition operators.

Note that the half-space *ssHL* process 4.2.2 is uniquely defined, but the half-space Yang-Baxter random field can have different construction approaches. We consider constructing the half-space Yang-Baxter random field by certain Markov transition operators. Suppose that we have four kinds of Markov transition operators

forward, bulk transition operator: $\mathcal{U}_{x,y}^{\leftarrow}(\varkappa \rightarrow \nu | \lambda, \mu)$ with $\varkappa \prec \mu \prec \nu \succ \lambda \succ \varkappa$

backward, bulk transition operator: $\mathcal{U}_{x,y}^{\rightarrow}(\nu \rightarrow \varkappa | \lambda, \mu)$ with $\varkappa \prec \mu \prec \nu \succ \lambda \succ \varkappa$

forward, boundary transition operator: $\mathcal{U}_{x,y}^{\leftarrow}(\varkappa \rightarrow \nu | \lambda)$ with $\varkappa \prec \nu \succ \lambda \succ \varkappa$

backward, boundary transition operator: $\mathcal{U}_{x,y}^{\rightarrow}(\nu \rightarrow \varkappa | \lambda)$ with $\varkappa \prec \nu \succ \lambda \succ \varkappa$

satisfy two reversibility conditions:

$$(4.3.1) \quad \mathcal{U}_{x,y}^{\leftarrow}(\varkappa \rightarrow \nu | \lambda, \mu) \Pi(x; y) f_{\lambda/\varkappa}(x) g_{\mu/\varkappa}(y) = \mathcal{U}_{x,y}^{\rightarrow}(\nu \rightarrow \varkappa | \lambda, \mu) f_{\nu/\mu}(x) g_{\nu/\lambda}(y)$$

$$(4.3.2) \quad \mathcal{U}_{x,y}^{\leftarrow}(\varkappa \rightarrow \nu | \mu) \Pi(x; y) g_{\mu/\varkappa}(y) \mathcal{G}_{\varkappa}(x) = \mathcal{U}_{x,y}^{\rightarrow}(\nu \rightarrow \varkappa | \mu) f_{\nu/\mu}(x) \mathcal{G}_{\nu}(y).$$

and four normalization conditions:

$$(4.3.3) \quad \sum_{\nu} \mathcal{U}_{x,y}^{\leftarrow}(\varkappa \rightarrow \nu | \lambda, \mu) = 1, \quad \sum_{\varkappa} \mathcal{U}_{x,y}^{\rightarrow}(\nu \rightarrow \varkappa | \lambda, \mu) = 1,$$

$$(4.3.4) \quad \sum_{\nu} \mathcal{U}_{x,y}^{\leftarrow}(\varkappa \rightarrow \nu | \mu) = 1, \quad \sum_{\varkappa} \mathcal{U}_{x,y}^{\rightarrow}(\nu \rightarrow \varkappa | \mu) = 1.$$

That is to say, $\mathcal{U}_{x,y}^{\leftarrow}(\varkappa \rightarrow \nu | \lambda, \mu)$ encodes the probability of a forward transition $\varkappa \rightarrow \nu$ on the bulk conditioned on λ, μ , and $\mathcal{U}_{x,y}^{\leftarrow}(\varkappa \rightarrow \nu | \lambda)$ encodes the probability of a forward transition $\varkappa \rightarrow \nu$ on the diagonal conditioned on λ . Similarly, $\mathcal{U}_{x,y}^{\rightarrow}(\nu \rightarrow \varkappa | \lambda, \mu)$ and $\mathcal{U}_{x,y}^{\rightarrow}(\nu \rightarrow \varkappa | \lambda)$ describe the probability of the opposite move on the bulk and diagonal. See Figure 12 for an illustration. It is easy to prove that the half-space random field can be inductively sampled by the forward transition probability $\mathcal{U}_{x,y}^{\leftarrow}(\varkappa \rightarrow \nu | \lambda, \mu)$ and $\mathcal{U}_{x,y}^{\leftarrow}(\varkappa \rightarrow \nu | \lambda)$ under the

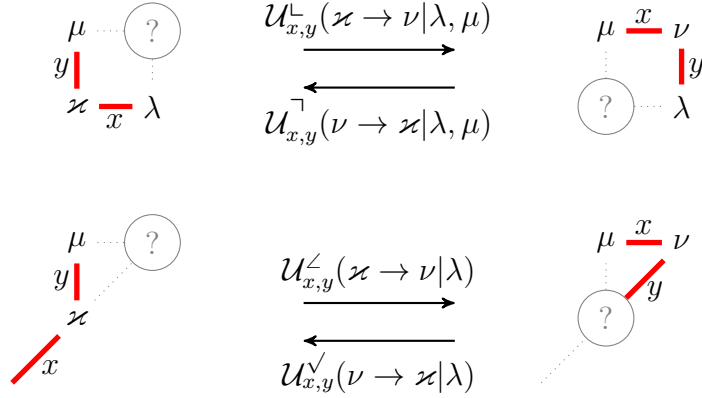


FIGURE 12. Top: Forward and backward, bulk transition operators. Bottom: Forward and backward, boundary transition operators.

empty boundary condition. We refer to [BBCS18, BP19, BBC20, BMP19, MP20] for more explanations. Particularly, summing both sides of 4.3.1 and 4.3.2 over \varkappa , we get the similar results of [BBCS18, Lemma 3.7, Lemma 3.8] and [BBC20, Lemma 2.7] by the normalization conditions 4.3.3 and 4.3.4.

4.4. Construction of the bulk transition operators. We construct the bulk transition operators \mathcal{U}^- and \mathcal{U}^+ by the bijectivisation of the Yang-Baxter equation introduced in [BP19]. The construction process is just the same as the procedure in [BMP19, Section 6]. For a convenience of the following content, let's briefly describe the procedure.

Note that we can represent the skew Cauchy identity (4.1.3) by the following partition function identity in the higher spin six vertex model with the vertices in Figure 1 and 3:

$$(4.4.1) \quad \Pi(x; y) \sum_{K_1, K_2, \dots \geq 0} \begin{array}{c} \infty \\ \uparrow \\ 1 \\ \text{---} \\ \infty \\ \downarrow \\ 0 \\ \infty \\ \downarrow \\ \infty \end{array} \begin{array}{c} J_1 \\ \uparrow \\ k_0 \\ \uparrow \\ K_1 \\ \downarrow \\ \ell_0 \\ \downarrow \\ I_1 \end{array} \begin{array}{c} J_2 \\ \uparrow \\ k_1 \\ \uparrow \\ K_2 \\ \downarrow \\ \ell_1 \\ \downarrow \\ I_2 \end{array} \dots \begin{array}{c} x \\ \nearrow \\ 0 \\ \searrow \\ 0 \\ \searrow \\ y \end{array} = \sum_{M_1, M_2, \dots \geq 0} \begin{array}{c} \infty \\ \downarrow \\ 0 \\ \downarrow \\ 1 \\ \downarrow \\ \infty \end{array} \begin{array}{c} J_1 \\ \downarrow \\ j_0 \\ \downarrow \\ M_1 \\ \uparrow \\ i_0 \\ \uparrow \\ I_1 \end{array} \begin{array}{c} J_2 \\ \downarrow \\ j_1 \\ \downarrow \\ M_2 \\ \uparrow \\ i_1 \\ \uparrow \\ I_2 \end{array} \dots \begin{array}{c} y \\ \nwarrow \\ 0 \\ \nwarrow \\ 0 \\ \nwarrow \\ x \end{array}$$

where we have used the notations:

$$(4.4.2) \quad \varkappa = 1^{K_1} 2^{K_2} \dots, \quad \lambda = 1^{J_1} 2^{J_2} \dots, \quad \mu = 1^{I_1} 2^{I_2} \dots, \quad \nu = 1^{M_1} 2^{M_2} \dots,$$

and we record the horizontal occupation numbers by sequences $\{k_h, \ell_h\}_{h \geq 0}$ for $f_{\mu/\varkappa}(x)g_{\lambda/\varkappa}(y)$, $\{i_h, j_h\}_{h \geq 0}$ for $f_{\nu/\lambda}(x)g_{\nu/\mu}(y)$.

The partition function identity (4.4.1) can be proved by applying the intertwining equation in the h -th column:

$$(4.4.3) \quad \sum_{0 \leq k_{h-1}, \ell_{h-1} \leq 1} \sum_{K_h \geq 0} \begin{array}{c} j_{h-1} \\ \nearrow \quad \searrow \\ i_{h-1} \end{array} \begin{array}{c} K_h \\ \uparrow \quad \downarrow \\ I_h \end{array} \begin{array}{c} k_{h-1} \quad k_h \\ \leftarrow \quad \rightarrow \\ \ell_{h-1} \quad \ell_h \end{array} \begin{array}{c} J_h \\ \leftarrow \quad \rightarrow \\ x \quad y \end{array} = \sum_{0 \leq k_1, k_3 \leq 1} \sum_{M_h \geq 0} \begin{array}{c} j_{h-1} \\ \nearrow \quad \searrow \\ i_{h-1} \end{array} \begin{array}{c} M_h \\ \uparrow \quad \downarrow \\ I_h \end{array} \begin{array}{c} j_h \quad k_h \\ \leftarrow \quad \rightarrow \\ \ell_h \end{array} \begin{array}{c} J_h \\ \leftarrow \quad \rightarrow \\ y \quad x \end{array}$$

where $i_{-1} = 1$, $j_{-1} = 0$, and $k_h = \ell_h = 0$ for all sufficiently large h . We also use the rotated vertices which we call R^* -vertex, and list their Boltzmann weights in Figure 13. See [BMP19, Figure 23, Proposition A.2].

$R^*(i, j; k, \ell)$	1	$\frac{1 - qxy}{1 - xy}$	$\frac{1 - q}{1 - xy}$	$\frac{(1 - q)xy}{1 - xy}$	$\frac{1 - qxy}{1 - xy}$	q

FIGURE 13. Boltzmann weight for R^* -vertex in (4.4.3)

We define two sets of configurations corresponding to the intertwining equation (4.4.3):

$$(4.4.4) \quad A_h = \left\{ a_h : a_h(k_{h-1}, \ell_{h-1}, K_h) = \begin{array}{c} j_{h-1} \\ \nearrow \quad \searrow \\ i_{h-1} \end{array} \begin{array}{c} K_h \\ \uparrow \quad \downarrow \\ I_h \end{array} \begin{array}{c} k_{h-1} \quad k_h \\ \leftarrow \quad \rightarrow \\ \ell_{h-1} \quad \ell_h \end{array} \begin{array}{c} J_h \\ \leftarrow \quad \rightarrow \\ x \quad y \end{array}, \quad 0 \leq k_{h-1}, \ell_{h-1} \leq 1, K_h \geq 0 \right\},$$

$$(4.4.5) \quad B_h = \left\{ b_h : b_h(i_h, j_h, M_h) = \begin{array}{c} j_{h-1} \\ \nearrow \quad \searrow \\ i_{h-1} \end{array} \begin{array}{c} M_h \\ \uparrow \quad \downarrow \\ I_h \end{array} \begin{array}{c} j_h \quad k_h \\ \leftarrow \quad \rightarrow \\ \ell_h \end{array} \begin{array}{c} J_h \\ \leftarrow \quad \rightarrow \\ y \quad x \end{array}, \quad 0 \leq i_h, j_h \leq 1, M_h \geq 0 \right\}.$$

where the boundary values $0 \leq i_{h-1}, j_{h-1}, k_h, \ell_h \leq 1$, $I_h, J_h \geq 0$ are fixed. Employing bijectivization of summation identities introduced in [BP19, Definition 2.1], we find a pair of local transition probability $(\mathbf{p}^{\text{fwd}}, \mathbf{p}^{\text{bwd}})$ in the h -th column which satisfy the following properties:

(1) The normalization condition for \mathbf{p}^{fwd} and \mathbf{p}^{bwd} :

$$(4.4.6) \quad \sum_{b_h \in B_h} \mathbf{p}^{\text{fwd}}(a_h, b_h) = 1 \text{ for all } a_h \in A_h, \quad \sum_{a_h \in A_h} \mathbf{p}^{\text{bwd}}(b_h, a_h) = 1 \text{ for all } b_h \in B_h.$$

(2) The reversibility condition between \mathbf{p}^{fwd} and \mathbf{p}^{bwd} :

$$(4.4.7) \quad w(a_h) \cdot \mathbf{p}^{\text{fwd}}(a_h, b_h) = w(b_h) \cdot \mathbf{p}^{\text{bwd}}(b_h, a_h) \quad \text{for all } a_h \in A_h, b_h \in B_h.$$

where $w(\cdot)$ means the Boltzmann weights of the configurations in A_h or B_h .

One can naturally construct the bulk transition probability $\mathcal{U}_{x,y}^{\perp}(\varkappa \rightarrow \nu | \lambda, \mu)$ and $\mathcal{U}_{x,y}^{\top}(\nu \rightarrow \varkappa | \lambda, \mu)$ by the product of the local transition probability:

$$(4.4.8) \quad \mathcal{U}_{x,y}^{\perp}(\varkappa \rightarrow \nu | \lambda, \mu) = \prod_{h=0}^{\infty} \mathbf{p}^{\text{fwd}}(a_h, b_h), \quad \mathcal{U}_{x,y}^{\top}(\nu \rightarrow \varkappa | \lambda, \mu) = \prod_{h=0}^{\infty} \mathbf{p}^{\text{bwd}}(b_h, a_h).$$

It is easy to check that the above construction satisfy the condition (4.3.1) and 4.3.3.

As an example, let us discuss of the local transition probability in the first column:

Example 4.3. Consider the configuration sets in the first column of (4.4.1):

$$(4.4.9) \quad A_0 = \left\{ a_0 : a_0(1, 0, \infty) = \begin{array}{c} \begin{array}{ccc} & \infty & x \\ & \uparrow & \nearrow k_0 \\ 0 & & \\ & \downarrow & \searrow \ell_0 \\ & \infty & y \end{array} \end{array} \right\},$$

$$(4.4.10) \quad B_0 = \left\{ b_0 : b_0(i_0, j_0, \infty) = \begin{array}{c} \begin{array}{ccc} y & \infty & \\ \uparrow & \downarrow & \\ 0 & & j_0 \\ & \downarrow & \searrow k_0 \\ & \infty & \\ & \uparrow & \nearrow \ell_0 \\ & \infty & \\ & \downarrow & \searrow \\ & \infty & x \end{array} \end{array}, 0 \leq i_0, j_0 \leq 1 \right\}.$$

where the boundary values $0 \leq k_0, \ell_0 \leq 1$ are fixed. We find that the set A_0 has a single element, the set B_0 has at most two elements, and the local transition probability is uniquely determined by:

$$\mathbf{p}^{\text{fwd}}(a_0(1, 0, \infty), b_0(i_0, j_0, \infty)) = \frac{M_{y,s}^*(\infty, 0; \infty, j_0) L_{x,s}(\infty, 1; \infty, i_0) R_{xy}^*(i_0, j_0; k_0, \ell_0)}{R_{xy}^*(1, 0; 1, 0) M_{y,s}^*(\infty, 0; \infty, \ell_0) L_{x,s}(\infty, 1; \infty, k_0)},$$

$$\mathbf{p}^{\text{bwd}}(b_0(i_0, j_0, \infty), a_0(1, 0, \infty)) = 1.$$

Further, if we set $k_0 = 0$ and $\ell_0 = 0$,

$$\mathbf{p}^{\text{fwd}}(a_0(1, 0, \infty), b_0(0, 0, \infty)) = \frac{1 - xy}{1 - qxy}, \quad \mathbf{p}^{\text{fwd}}(a_0(1, 0, \infty), b_0(1, 1, \infty)) = \frac{(1 - q)xy}{1 - qxy}.$$

If we set $k_0 = 1$ and $\ell_0 = 1$,

$$\mathbf{p}^{\text{fwd}}(a_0(1, 0, \infty), b_0(0, 0, \infty)) = \frac{1 - q}{1 - qxy}, \quad \mathbf{p}^{\text{fwd}}(a_0(1, 0, \infty), b_0(1, 1, \infty)) = \frac{q(1 - xy)}{1 - qxy}.$$

If we set $k_0 = 0, \ell_0 = 1$ or $k_0 = 1, \ell_0 = 0$,

$$\mathbf{p}^{\text{fwd}}(a_0(1, 0, \infty), b_0(0, 1, \infty)) = \mathbf{p}^{\text{fwd}}(a_0(1, 0, \infty), b_0(1, 0, \infty)) = 1.$$

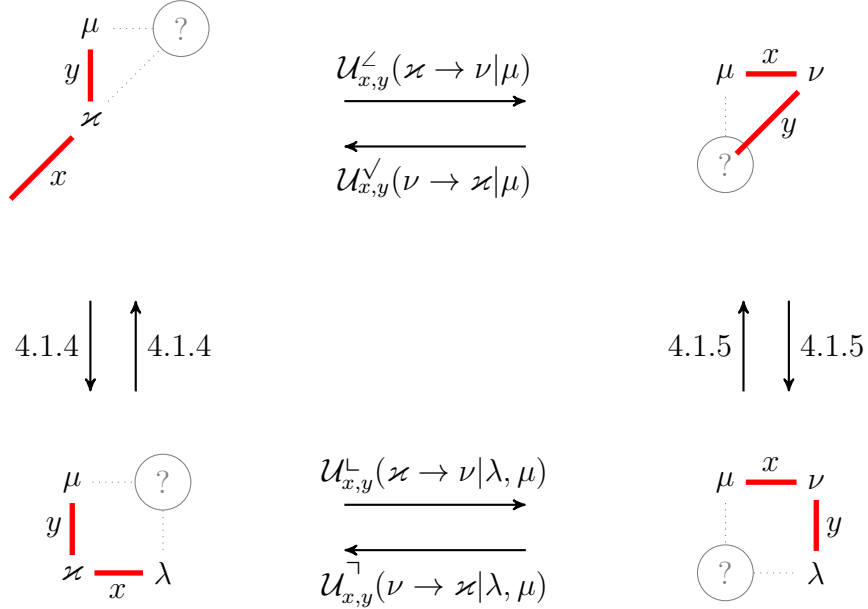


FIGURE 14. The boundary transition operators $\mathcal{U}^{<}$ and $\mathcal{U}^{>}$ are constructed by the bulk transition operators \mathcal{U}^{-} and \mathcal{U}^{+} , where the partition λ has even transport.

4.5. **Construction of the boundary transition operators.** Thanks to the skew Littlewood identity (4.1.4) introduced in the skew Cauchy-Littlewood structure, one can determine the boundary transition operators $\mathcal{U}^{<}$ and $\mathcal{U}^{>}$ by the bulk transition operators \mathcal{U}^{-} and \mathcal{U}^{+} . We perform the construction of $\mathcal{U}_{x,y}^{<}(\varkappa \rightarrow \nu|\mu)$ in the following procedure:

- (1) For a given partition \varkappa , we determine a unique partition λ such that

$$\mathbb{1}_{\tau' \text{ even}} b_{\tau}^{el} g_{\varkappa/\tau}(x) = \mathbb{1}_{\lambda' \text{ even}} b_{\lambda}^{el} f_{\lambda/\varkappa}(x)$$

- (2) Conditioned on the partitions μ and λ , we sample the random partition ν according to $\mathcal{U}_{x,y}^{-}(\varkappa \rightarrow \nu|\lambda, \mu)$.

And we perform the construction of $\mathcal{U}_{x,y}^{>}(\nu \rightarrow \varkappa|\mu)$ in the following procedure:

- (1) For a given partition ν , we determine a unique partition λ such that

$$\lambda' \text{ is even and } \lambda \prec \nu.$$

- (2) Conditioned on the partitions μ and λ , we sample the random partition \varkappa according to $\mathcal{U}_{x,y}^{+}(\nu \rightarrow \varkappa|\lambda, \mu)$.

See Figure 14 for an illustration. It is easy to check that the boundary transition operators constructed in Figure 14 satisfy (4.3.2) and 4.3.4. Obviously, from the above construction process, the sampling of ν in $\mathcal{U}_{x,y}^{<}(\varkappa \rightarrow \nu|\mu)$ depends on the starting partition \varkappa , but the push-block dynamics in [BBCS18, BBC20] do not have this property.

4.6. Evolution of the lengths of the partitions. We can find that the evolution of the lengths of partitions in the half-space random field is just the Markov projection of the forward transition onto the first column. We refer to [BP19, BMP19, MP20] for the definition of Markov projection.

In fact, we observe that the horizontal occupation numbers i_0, j_0, k_0, ℓ_0 in (4.4.1) encode the evolution of the length of partitions:

$$(4.6.1) \quad k_0 = \ell(\lambda) - \ell(\varkappa), \quad \ell_0 = \ell(\mu) - \ell(\varkappa); \quad i_0 = \ell(\nu) - \ell(\mu), \quad j_0 = \ell(\nu) - \ell(\lambda);$$

That means the evolution of the lengths of partitions on the bulk can be determined by local transition probability in Example 4.3, we list them in Figure 15.

Following the construction in Figure 14, once we determine the length of partition λ , the length of partition ν can be determined by the evolution in Figure 15. See Example 4.1 for an illustration, we can determine the length of λ by the length of \varkappa :

$$\ell(\lambda) = \begin{cases} \ell(\varkappa), & \ell(\varkappa) \text{ is even,} \\ \ell(\varkappa) + 1, & \ell(\varkappa) \text{ is odd.} \end{cases}$$

That means we can get the evolution of the lengths of partitions on the boundary in Figure 16 and Figure 17.

$\frac{1-xy}{1-qxy}$	$\frac{(1-q)xy}{1-qxy}$	$\frac{1-q}{1-qxy}$	$\frac{q(1-xy)}{1-qxy}$	1	1

FIGURE 15. Evolution of the lengths of partitions on the bulk.

$\frac{1-xy}{1-qxy}$	$\frac{(1-q)xy}{1-qxy}$	1

FIGURE 16. Evolution of lengths of partitions on the boundary as ℓ is even.

$\frac{1-q}{1-qxy}$	$\frac{q(1-xy)}{1-qxy}$	1

FIGURE 17. Evolution of the lengths of partitions on the boundary if ℓ is odd.

4.7. A dynamic stochastic six vertex model in a half-quadrant. Let us consider the half-quadrant $\{(i, j) \in \mathbb{Z}_{>0}^2 : i \leq j\}$. We assign a bulk vertex in Figure 18 at each point $(i, j) \in \mathbb{Z}_{>0}^2$ such that $i < j$, while the points $(i, i) \in \mathbb{Z}_{>0}^2$ are occupied by corner vertices in Figure 19 and 20, where we have used the following notation to simplify:

$$b_{ij} = \frac{q(1 - x_{i-1}x_j)}{1 - qx_{i-1}x_j}, \quad c_{ij} = \frac{1 - x_{i-1}x_j}{1 - qx_{i-1}x_j}.$$

Connecting each vertex configuration, we get an ensemble of up-right paths in the half-quadrant. Fix a configuration of up-right paths, we define the height function $h(i, j)$ for any given point (i, j) to be the number of paths that crossing one of the point $(k, j + 0.5)$ for $1 \leq k \leq i$. See Figure 21 for an illustration, where we set $h(0, j) = 0$ for $j \geq 0$, and we label the height function $h(i, j)$ at position $(i + 0.5, j + 0.5)$.

1	b_{ij}	$1 - b_{ij}$	c_{ij}	$1 - c_{ij}$	1

FIGURE 18. Bulk vertex at (i, j) , evolution of height function and the sampling probability.

c_{ii}	$1 - c_{ii}$	1	0

FIGURE 19. Corner vertex at (i, i) , evolution of height function and the sampling probability as h is even.

b_{ii}	$1 - b_{ii}$	1	0

FIGURE 20. Corner vertex at (i, i) , evolution of height function and the sampling probability if h is odd.

Definition 4.4. Fix $q \in (0, 1)$ and a sequence of parameters x_0, x_1, \dots such that $0 < x_i x_j < 1$ for all $0 \leq i < j$. The dynamic stochastic six vertex model in a half-quadrant (*DS6V in a half-quadrant for short*) is a probability measure on an ensemble of the up-right paths defined inductively as follows:

- At each vertex $(1, j)$, $j \in \mathbb{Z}_{\geq 1}$, there is a new path enters through the left boundary of the half-quadrant.

- Assume that the path configurations below the line $i + j \leq n$ (for some $n \in \mathbb{Z}_{\geq 2}$) are all determined. Thus, we know the incoming configuration of paths at vertices $\{(i, j)\}_{i+j=n}$ and the values of the height function at each point $(i, j) \in \mathbb{Z}_{\geq 0}$, with $i + j \leq n$. Using the probabilities in Figures 18–20 to sample the outgoing configuration of paths at vertices $\{(i, j)\}_{i+j=n}$ independently, this determines the incoming path configurations of the vertices $\{(i, j)\}_{i+j=n+1}$.
- By induction on n , one can fill out the whole half-quadrant.

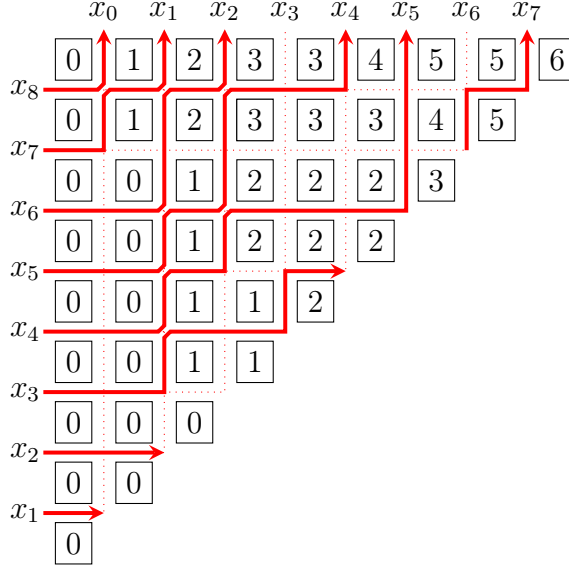


FIGURE 21. A path configuration in the half-quadrant with its height function.

Proposition 4.5. Let $\mathfrak{H} := \{h(i, j)\}_{j \geq i > 0}$ be the half-space random field of values of the height function of DS6V in a half-quadrant (Definition 4.4). Let $\lambda = \{\lambda^{(i, j)} : (i, j) \in \mathbb{H}\}$ be the half-space Yang-Baxter random field in Definition 4.2. Surely, the half-space random fields \mathfrak{H} and the half-space random field $\{\ell(\lambda^{(i, j)}) : (i, j) \in \mathbb{H}\}$ have the same distribution.

Proof. It is straightforward from the identification of weights in Figures 15–17 and the sampling probabilities in Figures 18–20, together with the identification of the boundary conditions. \square

The vertex model introduced in Definition 4.4 is different from the one introduced in [BBCW18, section 4.1]. Although both vertex models have the same bulk vertex configurations, the corner vertex configurations in Definition 4.4 are more complicated, and they depend on the height function. In the vertex model of [BBCW18, section 4.1], the height function $h(i, i)$ in the diagonal can only be even number. While, in Definition 4.4, the height function $h(i, i)$ in the diagonal can be else even or odd. Furthermore, the Proposition 4.5 can give us more information about the distribution of height function than [BBCW18, Theorem 4.4], and we do not need to perform the combinatorial calculation any more.

Using the difference operators for *ssHL functions* found in [BMP19, Theorem 8.2], we can derive the q -moments of the DS6V in a half-quadrant. The method is similar with the work

in [BBC20, Section 3]. However, the result is not directly amenable for asymptotic analysis, so we do not consider it here.

The DS6V in a half-quadrant can be naturally related to a dynamic version of discrete-time interacting particle system on the half-line with an open boundary. The method is similar to [BBCW18, Section 5]. The first step is to turn the ensemble of the paths introduced in Definition 4.4 into its complementation. This means that each edge state $0 \leq i \leq 1$ becomes a state $1 - i$ (See Figure 22 Left for example). The next step, we associate an evolution of particle configurations to the above complementation: denote the state at position i and time t by $\xi_i(t)$, let it be 1 if there is a path on the edge $(t - i + 1, t) \rightarrow (t - i + 1, t + 1)$, and 0 else (See Figure 22 Right). We defines the current at site x by

$$N_x(t) = \sum_{i=x}^{\infty} \xi_i(t)$$

and for a convenience, set the number of particles in the system on time t as $N(t) = N_1(t)$. The label of the positions of the $N(t)$ particles from right to left is

$$y_1 > y_2 > \cdots > y_{N(t)} > 0.$$

If $N(t) = 0$, here the convention that $y_0 = \infty$ is used. Note that $N(t) = t - h(t, t)$.

The particle configuration $(y_i)_{i \in \mathbb{Z}_{>0}}$ is a dynamic version of ASEP-type discrete-time interacting particle system which evolve according to the following rules:

- (1) For $1 \leq i \leq N(t)$, the i -th particle jumps by 1 at time $t + 1$ with probability $c_{t-y_i(t)+1, t+1}$, provided $y_{i-1}(t+1) > y_i(t) + 1$.
- (2) For $1 \leq i \leq N(t) - 1$, the i -th particle jumps by $-j$ at times $t + 1$ with probability
 - $(1 - c_{t-y_i(t)+1, t+1})(1 - b_{t-y_i(t)+j+2, t+1}) \prod_{k=1}^j b_{t-y_i(t)+k+1, t+1}$ as $y_{i-1}(t+1) > y_i(t) + 1$ well as $1 \leq j \leq y_i(t) - y_{i+1}(t) - 2$;
 - $(1 - b_{t-y_i(t)+j+2, t+1}) \prod_{k=1}^j b_{t-y_i(t)+k+1, t+1}$ as $y_{i-1}(t+1) = y_i(t) + 1$ well as $1 \leq j \leq y_i(t) - y_{i+1}(t) - 2$;
 - $(1 - c_{t-y_i(t)+1, t+1}) \prod_{k=1}^j b_{t-y_i(t)+k+1, t+1}$ as $y_{i-1}(t+1) > y_i(t) + 1$ well as $j = y_i(t) - y_{i+1}(t) - 1$;
 - $\prod_{k=1}^j b_{t-y_i(t)+k+1, t+1}$ as $y_{i-1}(t+1) = y_i(t) + 1$ well as $j = y_i(t) - y_{i+1}(t) - 1$;
- (3) If the leftmost particle lies at site $y_{N(t)}(t) > 2$, it jumps by $-j$ at times $t + 1$ with probability
 - $(1 - c_{t-y_i(t)+1, t+1})(1 - b_{t-y_i(t)+j+2, t+1}) \prod_{k=1}^j b_{t-y_i(t)+k+1, t+1}$ as $y_{N(t)-1}(t+1) > y_{N(t)}(t) + 1$ well as $1 \leq j \leq y_{N(t)}(t) - 2$;
 - $(1 - b_{t-y_i(t)+j+2, t+1}) \prod_{k=1}^j b_{t-y_i(t)+k+1, t+1}$ as $y_{N(t)-1}(t+1) = y_{N(t)}(t) + 1$ well as $1 \leq j \leq y_{N(t)}(t) - 2$;
it jumps to the site 1 with probability (set $j = y_{N(t)}(t) - 1$)
 - $(1 - c_{t-y_i(t)+1, t+1})(1 - b_{t-y_i(t)+j+2, t+1}) \prod_{k=1}^j b_{t-y_i(t)+k+1, t+1}$ as $t - N(t) = t - N_2(t + 1) - 1$ is odd well as $y_{N(t)-1}(t+1) > y_{N(t)}(t) + 1$;
 - $(1 - c_{t-y_i(t)+1, t+1}) \prod_{k=1}^j b_{t-y_i(t)+k+1, t+1}$ as $t - N(t) = t - N_2(t + 1) - 1$ is even well as $y_{N(t)-1}(t+1) > y_{N(t)}(t) + 1$;
 - $(1 - b_{t-y_i(t)+j+2, t+1}) \prod_{k=1}^j b_{t-y_i(t)+k+1, t+1}$ as $t - N(t) = t - N_2(t + 1) - 1$ is odd well as $y_{N(t)-1}(t+1) = y_{N(t)}(t) + 1$;

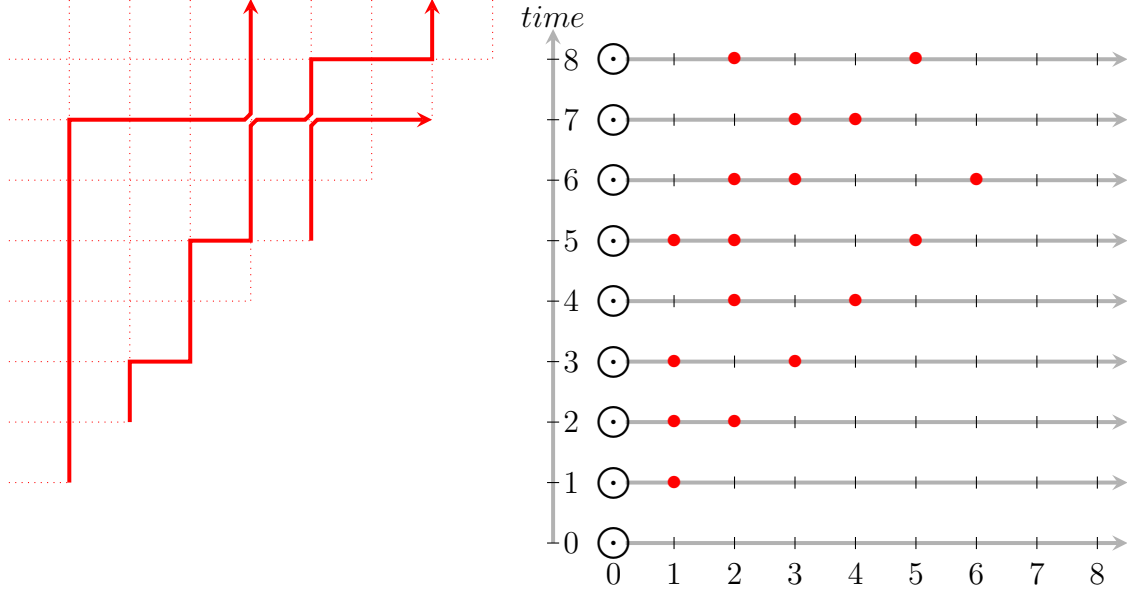


FIGURE 22. Left: the same path configuration as in Figure 21 after particle-hole transformation. Right: corresponding particle configurations. There is a reservoir at site 0, a particle may be injected at site 1 or be removed from the system in the next step.

- $\prod_{k=1}^j b_{t-y_i(t)+k+1,t+1}$ as $t - N(t) = t - N_2(t+1) - 1$ is even well as $y_{N(t)-1}(t+1) = y_{N(t)}(t) + 1$.
- (4) If $y_{N(t)}(t+1) > 1$, a new particle is created at site 1 with probability
- c_{tt} as $t - N(t) = t - N_2(t+1)$ is even;
 - 1 as $t - N(t) = t - N_2(t+1) - 1$ is even;
 - $1 - b_{tt}$ as $t - N(t) = t - N_2(t+1) - 1$ is odd;
 - 0 as $t - N(t) = t - N_2(t+1)$ is odd.
- (5) If $t - N(t) = t - N_2(t+1) - 1$ is odd and $0 < y_{N(t)}(t) = j < \infty$, this particle ejects from the system at time $t+1$, happening with probability
- $(1 - c_{t-j+1,t+1}) \prod_{k=t-j+2}^{t+1} b_{k,t+1}$ as $y_{N(t)-1}(t+1) > j+1$;
 - $\prod_{k=t-j+2}^{t+1} b_{k,t+1}$ as $y_{N(t)-1}(t+1) = j+1$.
 - 0 if $t - N(t) = t - N_2(t+1) - 1$ is even.
- (6) Each particle stays put with complementary probability.

REFERENCES

- [ABW21] A. Aggarwal, A. Borodin, and M. Wheeler. Colored Fermionic Vertex Models and Symmetric Functions. *Preprint, arXiv:2101.01605*.
- [Bax82] R.J. Baxter. Exactly solved models in statistical mechanics. Academic Press, Inc. (Harcourt Brace Jovanovich, Publishers), London, 1982.
- [BBC20] G. Barraquand, A. Borodin, and I. Corwin. Half-space Macdonald processes. *Forum of Mathematics, Pi*, 8:e11, 2020. *arXiv:1802.08210*.
- [BBCS18] J. Baik, G. Barraquand, I. Corwin, and T. Suidan, Pfaffian schur processes and last passage percolation in a half-quadrant, *Ann. Probab.*, 46:3015–3089, 2018. *arXiv:1606.00525*

- [BBCW18] G. Barraquand, A. Borodin, I. Corwin, and M. Wheeler, Stochastic six-vertex model in a half-quadrant and half-line open asymmetric simple exclusion process, *Duke Mathematical Journal*, 167:2457–2529, 2018. *arXiv:1704.04309*.
- [BBW16] A. Borodin, A. Bufetov, and M. Wheeler, Between the stochastic six vertex model and Hall-Littlewood processes. *To appear in Journal of Combinatorial Theory Series A*. *arXiv:1611.09486*.
- [BC14] A. Borodin, I. Corwin. Macdonald processes. *Probab. Theory Relat. Fields*, 158:225–400, 2014. *arXiv:1111.4408*.
- [Bor17] A. Borodin. On a family of rational symmetric functions. *Adv. Math.*, 306:973–1018, 2017. *arXiv:1410.0976*.
- [Bor18] A. Borodin. Stochastic higher spin six vertex model and Macdonald measures. *Jour. Math. Phys.*, 59(2):023301, 2018. *arXiv:1608.01553*.
- [BMP19] A. Bufetov, M. Mucciconi, and L. Petrov. Yang-Baxter random fields and stochastic vertex models. *To appear in Adv. Math.* *arXiv:1905.06815*.
- [BP18] A. Borodin and L. Petrov. Higher spin six vertex model and rational symmetric functions. *Selecta Math.*, 24(2):751–874, 2018. *arXiv:1601.05770*.
- [BP16] A. Borodin and L. Petrov. Lectures on Integrable probability: Stochastic vertex models and symmetric functions. In *Stochastic processes and random matrices*, page 26-131. Oxford Univ. Press, Oxford, 2017. *arXiv:1605.01349*.
- [BP19] A. Bufetov and L. Petrov. Yang-Baxter field for spin Hall-Littlewood symmetric functions. *Forum Math. Sigma*, 7:e39, 2019. *arXiv:1712.04584*.
- [BW20] A. Borodin and M. Wheeler. Spin q -whittaker polynomials. *Adv. Math.* 2020, <https://doi.org/10.1016/j.aim.2020.107449>. *arXiv:1701.06292*.
- [BW18] A. Borodin and M. Wheeler. Coloured stochastic vertex models and their spectral theory. *preprint arXiv:1808.01866*.
- [CP16] I. Corwin and L. Petrov. Stochastic higher spin vertex models on the line. *Commun. Math. Phys.*, 343(2):651–700, 2016. *arXiv:1502.07374*.
- [Cue18] C. Cuenca. Interpolation macdonald operators at infinity. *Advances in Applied Mathematics*, 101:15-59, 2018. *arXiv:1712.08014*.
- [Dim18] E. Dimitrov. Six-vertex Models and the GUE-corners Process. *Intern. Math. Research Notices*, 2018. *arXiv:1610.06893*.
- [Gav21] S. Gavrilova. Refined Littlewood identity for spin Hall-Littlewood rational functions. *Preprint, arXiv:2104.09755*.
- [GdGW17] A. Garbali, J. de Gier, and M. Wheeler. A new generalisation of Macdonald polynomials. *Comm. Math. Phys.*, 352(2):773–804, 2017. *arXiv:1605.07200*.
- [Kor21] S. Korotkikh. Hidden diagonal integrability of q -Hahn vertex model and beta polymer model. *Preprint, arXiv:2105.05058*.
- [KPZ86] K. Kardar, G. Parisi, Y.Z. Zhang. Dynamic scaling of growing interfaces. *Phys. Rev. Lett.* 56, pp 889-892, 1986.
- [Mac95] I.G. Macdonald. Symmetric functions and Hall polynomials. Oxford University Press, 2nd edition, 1995.
- [MP20] M. Mucciconi, L. Petrov. Spin q -Whittaker polynomials and deformed quantum Toda. *Preprint, arXiv:2003.14260*.
- [Ols19] G. Olshanski. Interpolation macdonald polynomials and cauchy-type identities. *Jour. Comb. Th. A*, 162:65-117, 2019. *arXiv:1712.08018*.
- [OP17] D. Orr and L. Petrov. Stochastic higher spin six vertex model and q -TASEPs. *Adv. Math.*, 317:473–525, 2017. *arXiv:1610.10080*.
- [Pet20] L. Petrov. Refined Cauchy identity for spin Hall-Littlewood rational symmetric functions. *Preprint, arXiv:2007.10886*.
- [WZJ16] M. Wheeler and P. Zinn-Justin. Refined Cauchy/Littlewood identities and six-vertex model partition functions: III. Deformed bosons. *Adv. Math.*, 299:543–600, 2016. *arXiv:1508.02236*.

INSTITUTE OF APPLIED MATHEMATICS, ACADEMY OF MATHEMATICS AND SYSTEMS SCIENCE, CHINESE
ACADEMY OF SCIENCES, AND THE UNIVERSITY OF CHINESE ACADEMY OF SCIENCES, BEIJING, CHINA.
Email address: chenkailun16@mails.ucas.ac.cn

INSTITUTE OF APPLIED MATHEMATICS, ACADEMY OF MATHEMATICS AND SYSTEMS SCIENCE, CHINESE
ACADEMY OF SCIENCES, BEIJING, CHINA.
Email address: xmding@amss.ac.cn